NASA TECHNICAL NOTE

NASA TN D-5912

NASA TN D-5912

THE USE OF LUNAR BEACONS IN LUNAR ORBIT ESTIMATION

by Thomas M. Carson

Ames Research Center

Moffett Field, Calif. 94035

1. Report No. NASA TN D-5912	2. Government Accession No.	3. Recipient's Catalog No.
4. Title and Subtitle THE USE OF LUNAR BEACONS IN LUNAR ORBIT ESTIMATION		5. Report Date August 1970
		6. Performing Organization Code
7. Author(s) Thomas M. Carson		8. Performing Organization Report No. A-3521
9. Performing Organization Name and Address NASA Ames Research Center Moffett Field, Calif., 94035		10. Work Unit No. 125-17-05-01-00-21
		11. Contract or Grant No.
12. Sponsoring Agency Name and Address National Aeronautics and Space Administration Washington, D. C. 20546		13. Type of Report and Period Covered Technical Note
		14. Sponsoring Agency Code

15. Supplementary Notes

16. Abstract

    Kalman filtering techniques were applied in evaluating the use of lunar beacons in estimating the state of a lunar vehicle. Range and/or range-rate measurements were used as the observational data.

    Results show that the error in the beacon location can be reduced from an initial error of 1.73 kilometers to approximately 0.2 kilometer, by the use of earth-based observations. The use of on-board observations of the lunar beacons can contribute significantly to lunar orbit estimation when used in conjunction with earth-based observations. Locating the beacons to provide state information that was difficult to obtain from earth-based measurements provided beneficial. On-board observations also proved adequate in estimating the state of a lunar vehicle when they were the only data source available.

17. Key Words (Suggested by Author(s)) Kalman Filtering State estimation On-board observation Lunar orbit estimation Observations of lunar beacons	18. Distribution Statement Unclassified - Unlimited		
19. Security Classif. (of this report) Unclassified	20. Security Classif. (of this page) Unclassified	21. No. of Pages 52	22. Price* $3.00

*For sale by the Clearinghouse for Federal Scientific and Technical Information
Springfield, Virginia 22151

TABLE OF CONTENTS

Page

SYMBOLS

a	semimajor axis of lunar satellite orbit
$\hat{D}_b$	down unit vector at beacon
$\hat{D}_s$	down unit vector at station
$\hat{E}_b$	east unit vector at beacon
$\hat{E}_s$	east unit vector at station
e	eccentricity of lunar satellite orbit
H	matrix relating observations to state
I	identity matrix
i	inclination of orbit plane of lunar satellite with respect to lunar equator
K	weighting matrix
$\hat{N}_b$	north unit vector at beacon
$\hat{N}_s$	north unit vector at station
P(t)	covariance matrix of estimation errors
Q	covariance matrix of measurement error
$\overline{RB}$	vector from center of moon to beacon
$\overline{RM}$	vector from center of earth to center of moon
$\overline{RS}$	vector from center of earth to station
$\bar{r}$	position vector of satellite with respect to center of moon
x,y,z,	inertial, selenocentric coordinate system (The x axis is positive in the direction of the mean vernal equinox of 1950.0. The z axis is normal to the mean equator of 1950.0 and positive in the northern hemisphere. The y axis forms a right-handed system with x and z.)
λ	longitude

μ	gravitational constant of the moon
ρ	range
$\dot{\rho}$	range rate
$\bar{\rho}$	range vector from station to satellite
$\dot{\bar{\rho}}$	velocity vector of satellite with respect to station
ρ_{ob}	on-board range
$\dot{\rho}_{ob}$	on-board range rate
$\bar{\rho}_{ob}$	range vector from satellite to beacon
$\dot{\bar{\rho}}_{ob}$	velocity vector of beacon with respect to satellite
$\Phi(t_j,t_i)$	transition matrix (relates state at time t_j to state at time t_i)
ϕ	latitude
Ω	longitude of the ascending node of satellite orbit plane
ω	argument of perigee for lunar satellite

Superscripts

T	transpose of a matrix
-1	inverse of a matrix
$(\dot{\ })$	derivative with respect to time
$(\hat{\ })$	unit vector
$(\bar{\ })$	vector

THE USE OF LUNAR BEACONS IN LUNAR ORBIT ESTIMATION

Thomas M. Carson

Ames Research Center

SUMMARY

Kalman filtering techniques were applied in evaluating the use of lunar beacons in estimating the state of a lunar vehicle. Range and/or range-rate measurements were used as the observational data. The following questions were considered:

1. Using range and range-rate observations from the Earth, how accurately can the location of a lunar beacon be determined?

2. Given some set of accuracies for earth-based radars, what relative accuracy would be required for on-board observations of lunar beacons to prove beneficial for state estimation?

3. How well can subsidiary uncertainties, that is, uncertainties other than those in position and velocity, be estimated?

4. Assuming that on-board observations of lunar beacons are beneficial, what would be the best locations for the beacons?

5. Assuming that only the on-board radar observations are available how well can the lunar orbit be estimated?

Results show that the error in the beacon location can be reduced from an initial error of 1.73 kilometers to approximately 0.2 kilometer, by the use of earth-based observations. The use of on-board observations of the lunar beacons can contribute significantly to lunar orbit estimation when used in conjunction with earth-based observations. Locating the beacons to provide state information that was difficult to obtain from earth-based measurements proved beneficial. On-board observations also proved adequate in estimating the state of a lunar vehicle when they were the only data source available.

INTRODUCTION

The advent of exploratory lunar missions has generated considerable interest in determining how accurately the trajectory of a space vehicle in lunar orbit can be estimated. Because of the lack of good angular data from earth-based radars, difficulties can be encountered in lunar orbit estimation when only earth-based data are available. One possible way to improve this situation is to make on-board radar observations of beacons located on the moon. "Beacons" are defined in this report as any type of device capable, in conjunction with electronic apparatus on board the vehicle, of generating range and/or range-rate information. The specific form of the device (e.g., simple

reflector or transponder) is immaterial to this study. It is assumed here that one or more such devices would be located on or near the lunar track so as to provide reasonable periods of tracking from the orbiting vehicle. These beacons would presumably have been placed on the lunar surface in a previous mission (or missions) and their precise locations determined as accurately as possible using information from the landing mission and/or direct tracking of the beacons from earth-based stations.

Because errors in the knowledge of the beacon locations are expected to have a significant effect on the utility of the beacons, the first question considered in the report is:

1. Using range and range-rate observations from the earth, how accurately can the location of a lunar beacon be determined?

To determine the utility of the beacons, the following questions are then considered:

2. Given some set of accuracies for earth-based radars, what relative accuracy would be required for on-board observations of lunar beacons to prove beneficial?

3. How well can subsidiary uncertainties (i.e., uncertainties other than those in position and velocity) be estimated?

4. Assuming that on-board observations of lunar beacons are beneficial, what would be the best locations for the beacons?

5. Assuming that only the on-board radar observations are available, how well can the lunar orbit be estimated?

The Kalman filter theory is used as a basis for evaluating the estimation performance. The application of this theory to the problem of space vehicle trajectory estimation (refs. 1-3) is summarized briefly in the report. Basically, what is required in the application is (1) specify the state variables, (2) write the state differential equations and measurement equations, (3) linearize these equations with respect to a reference orbit, and (4) use the theory to develop the variance equations, whose solution gives the estimation performance.

For the results of the study to be realistic the process of specifying the state variables must involve identifying all those quantities whose uncertainties are expected to contribute significant errors. Thus, besides the state of the vehicle itself (i.e., its position and velocity) certain so-called subsidiary variables are included in the estimation problem, and the covariance matrix obtained as the solution of the variance equation indicates not only how well the vehicle trajectory is determined, but also the improvement in estimation accuracy obtained simultaneously for the subsidiary variables. The subsidiary variables in the present study include station location errors, beacon location errors, measurement errors, and timing errors.

The reference orbit used in this report is obtained by numerically integrating the orbital equations of motion. The numerical integration scheme is described in reference 4. The equations of motion include the moon as the central body and the earth and sun as perturbing bodies. The lunar potential is expressed as a triaxial ellipsoid.

The results obtained apply to only one particular orbit. Obviously, if other orbits were selected, results would differ from those in this report. In general, however, the information obtained in this report would be true for other orbits. The orbit considered is the September 17, 1969, reference orbit for the Command Service Module lunar parking orbit of the Apollo mission. This particular orbit was chosen because it was associated with an actual project. Also, the orbit's geometry with respect to the earth is such as to introduce the problems of observability when only earth-based measurements are available.

THE PROBLEM FORMULATION

To use the Kalman filter theory as a basis of evaluating the estimation performance, the following parts are required:

1. The filter equations.

2. The reference trajectory.

3. The observation equations.

4. The partial derivatives which relate the observations to the state.

5. In this problem where an attempt is made to locate the beacons to provide maximum information about the elements that are poorly defined from earth-based trackers, the location of these beacons must be determined.

Each of these items will be considered in the following sections.

The Filter Equations

As mentioned in the Introduction, it is desired to consider both observations of a lunar orbiting vehicle from earth-based stations and observations of lunar beacons from on-board the vehicle. Evaluation of the information content of these observations will indicate how well the state of the vehicle, plus certain other uncertain parameters in the problem, can be estimated.

The data-processing scheme assumed in this report is of the recursive, minimum-variance type (i.e., a Kalman filter). Since the theory applies strictly to linear systems only and since the problem is nonlinear, it is assumed that the equations governing the vehicle motion and the observations can be successfully linearized. That is, the filter processes deviation data to estimate deviations from a reference trajectory, and it is assumed that the reference plus estimated deviation is a true representation of the "best" (minimum variance) estimate of the trajectory.

Since this report is concerned only with an error analysis, no actual trajectory is considered, and only the variance equations of the filter need be implemented. These variance equations (derived in refs. 1-3) are as follows, assuming discrete time observations. Between two observations the covariance matrix of estimation errors in $x(t)$, the deviation state vector, is updated by the

3

equation

$$P(t_i) = \Phi(t_i,t_0)P(t_0)\Phi^T(t_i,t_0) \tag{1}$$

where $\Phi(t_i,t_0)$ is the transition matrix which relates conditions at t_i to conditions at t_0. That is, the system equations are of the form $x(t_i) = \Phi(t_i,t_0)x(t_0)$. (Note that no random forcing function is assumed; that is, the vehicle is on an unperturbed "free-fall" trajectory.) When an observation or set of observations at time t are processed to improve the state vector estimate, the equation employed is

$$P_a(t) = (I - KH)P_b(t)(I - KH)^T + KQK^T \tag{2}$$

where

$P_a(t)$ is covariance of state errors after the observation has been processed

$P_b(t)$ is covariance of state errors before the observation has been processed

H   is the matrix of partial derivatives of the observed quantities with respect to the state variables

$K = PH^T(HPH^T + Q)^{-1}$

Q   is the covariance matrix of observation errors

I   is the identity matrix

Generation of Reference Trajectory

The generation of a reference trajectory is the process of computing the vehicle's postion and velocity at any later time, given its position and velocity at some initial time. This may be accomplished by numerically integrating a set of differential equations expressed in an inertial coordinate system. How well the reference trajectory is determined depends on how accurately the equations of motion are described.

In this report, these equations are expressed in a three-dimensional rectangular selenocentric inertial coordinate system. The positive x axis of this system points in the direction of the mean vernal equinox of 1950.0. The z axis is normal to the mean equatorial plane of 1950.0, positive in the northern hemisphere, and the y axis forms a right-handed system with x and z. These orbital equations include the gravitational effects of the earth, sun, and moon. The earth and sun are treated as point masses and the lunar potential function is expressed as a triaxial ellipsoid. The ephemerides of the sun and moon with respect to the earth in a 1950.0 frame are available on magnetic tape obtained from the Jet Propulsion Laboratory. These equations are integrated numerically with a subroutine described in reference 4. This subroutine is used intact and will not be described in this report.

The orbit considered in this report is the September 17,1969, reference orbit for the Command Service Module lunar parking orbit of the Apollo mission. The orbit is essentially circular
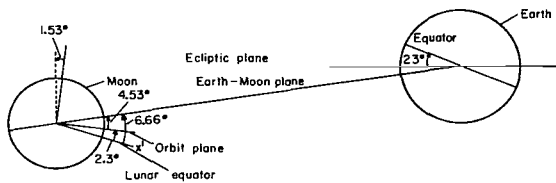
Sketch (a)

with a period of approximately 2 hours. The longitude of the node is 95° with respect to a selenocentric frame. The inclination of the orbit plane is 177° with respect to the selenocentric frame or approximately 4.5° with respect to the earth-moon plane (see sketch (a)). The orbital elements with respect to a selenocentric frame are:

a	1 894.552 km
e	0.0004648
i	177.67°
ω	279.12°
Ω	95.12°

Observations Types

Observations from three earth-based stations (Goldstone, Woomera, and Johannesburg) and from on-board the satellite are considered. For this analysis it is assumed that range-rate observations are taken every 5 minutes from the earth-based stations when the vehicle is in view. The vehicle is considered to be in view when it is 5° above the station horizon and is not occulted by the moon. Two relevant questions should be considered at this point: (1) Why not use both range and range-rate observations from earth-based radar? and (2) Why choose a 5-minute observation interval? In some preliminary work (ref. 5) both range and range-rate observations were considered and an improvement was seen by the addition of the range observations. However, this same improvement could be obtained by increasing the accuracy of the range-rate observations. It was felt, therefore, that the range observations did not contribute any new information that was not already available in the range-rate observations. The use of earth-based observations, either range or range-rate or both, in estimating the elements of a lunar satellite orbit is discussed in reference 6.

In practice, observation rates may be as frequent at every tenth of a second from earth-based radar. Obviously, the computations involved in such frequent observations would be too burdensome for this study; moreover, such frequent observations are unnecessary since an increased observation rate can be simulated by appropriately reducing the assumed observation noise. Three different sets of noise figures used in the report are given in the following table. The first noise figure, $\sigma_{\dot{\rho}} = 0.04$ m/s, was taken from a GSFC-MSC Apollo report. It is a fairly conservative figure, presumed to represent the noise level in range-rate measurements made once per second. When a 5-minute observation interval is used to simulate once per second observations the equivalent noise level is approximately 0.00012 m/s, which is the third entry in the table. The second numerical entry, 0.002 m/s, is chosen, more or less arbitrarily, between the other two to represent the degradation from ideal system performance which is likely to occur because of unmodeled observation error sequential correlation or other unmodeled system errors. The on-board noise figures were obtained in the same manner.

5

	Observation noise			
	Earth-based	On-board		
Case	$\sigma_{\dot{\rho}}$, m/s	σ_ρ, m	$\sigma_{\dot{\rho}}$, m/s	
1	0.04	30	0.3	
2	.002	4.8	.04	
3	.00012	1.0	.01	

The earth-based range-rate observations are computed in the following manner.

$$\dot{\rho} = \frac{\bar{\rho} \cdot \dot{\bar{\rho}}}{\rho}$$

where

$\bar{\rho}$ range vector from station to satellite

$\dot{\bar{\rho}}$ velocity vector of satellite with respect to station

ρ $(\bar{\rho} \cdot \bar{\rho})^{1/2}$

Range and range-rate observations are assumed to be taken from the lunar satellite to a beacon whenever the satellite is above the horizon of the beacon. Again, a 5-minute observation interval is employed in the simulation. These observations are computed as follows:

$$\rho_{ob} = (\bar{\rho}_{ob} \cdot \bar{\rho}_{ob})^{1/2}$$

$$\dot{\rho}_{ob} = \frac{\bar{\rho}_{ob} \cdot \dot{\bar{\rho}}_{ob}}{\rho_{ob}}$$

where

$\bar{\rho}_{ob}$ range vector from satellite to beacon

$\dot{\bar{\rho}}_{ob}$ velocity vector of beacon with respect to satellite

Partial Derivatives of Observations With Respect to State

As mentioned previously in the development, partial derivatives that relate the observations to the state vector are required. This is the H matrix shown in equation (2). The H matrix has as

many columns as variables in the state vector and has one row for each observation processed simultaneously. Since only one observation is processed at a time in the present program, the H matrix can be considered a row vector and be partitioned as follows:

$$H = \begin{bmatrix} H_X & | & H_S & | & H_B & | & H_T & | & H_b \end{bmatrix}$$

where

H_X is a 1X6 matrix relating the observation to vehicle position and velocity

H_S is a 1 X 3 matrix relating the observation to errors in station location

H_B is a 1X1 matrix relating the observation to bias in the observation

H_T is a 1X1 matrix relating the observation to observation timing error

H_b is a 1 X 3 matrix relating the observation to beacon location errors

The mathematical expressions for the partial derivatives taken from an unpublished Philco report that was written under Contract NAS 5-9700 are given below:

For earth-based range-rate observations

$$H_X = (1/\rho)\,[\,(\dot{\bar{\rho}} - \bar{\rho}\dot{\rho}/\rho) \;|\; \bar{\rho}\,]$$

$$H_S = -(1/\rho)\,[\dot{\bar{\rho}} + (\bar{\rho} \times \bar{\omega}_E) - \dot{\rho}\bar{\rho}/\rho]\,\cdot\,(\hat{N}_S \hat{E}_S \hat{D}_S)$$

$$H_B = 1$$

$$H_T = (1/\rho)\,[\,(\dot{\bar{\rho}} \cdot \dot{\bar{\rho}}) + \bar{\rho} \cdot \ddot{\bar{\rho}} - \dot{\rho}^2\,]$$

$$H_b = 0$$

For on-board range observations

$$H_X = -(1/\rho_{ob})\,(\bar{\rho}_{ob} \;|\; 0)$$

$$H_S = 0$$

$$H_B = 1$$

$$H_T = \dot{\rho}_{ob}$$

$$H_b = (1/\rho_{ob})\,[\bar{\rho}_{ob} \cdot (\hat{N}_b \hat{E}_b \hat{D}_b)]$$

7

For on-board range-rate observations

$$H_X = -(1/\rho_{ob}) \left\{ [\dot{\bar{\rho}}_{ob} - (\dot{\rho}_{ob}/\rho_{ob})\bar{\rho}_{ob}] \mid \bar{\rho}_{ob} \right\}$$

$$H_S = 0$$

$$H_B = 1$$

$$H_T = -(1/\rho_{ob}) [(\dot{\bar{\rho}}_{ob} \cdot \dot{\bar{\rho}}_{ob}) + \bar{\rho}_{ob} \cdot \ddot{\bar{\rho}}_{ob} - \dot{\rho}_{ob}^2]$$

$$H_b = (1/\rho_{ob}) [\dot{\bar{\rho}}_{ob} - (\dot{\rho}_{ob}\bar{\rho}_{ob}/\rho_{ob}) + (\bar{\rho}_{ob} \times \bar{\omega}_m)] \cdot (\hat{N}_b \hat{E}_b \hat{D}_b)$$

Location of Beacons

From preliminary work (ref. 5) it was found that two beacons would be a sufficient number for on-board observations if both range and range-rate observations were available. The first consideration in the choice of sites for these two beacons is that one should be on the far side of the moon since no earth-based tracking of the orbiting vehicle is available during this part of the orbit. The other beacon would be located on the front side. However, this is somewhat intuitive, and another factor which may influence the choice of sites is that a front-side beacon site can be expected to be known more accurately than one on the far side because of the possibility of direct earth-based tracking of the front-side beacon. This matter is considered in some detail later in the report.

It was shown in reference 6 that the orientation angles (i and Ω) are difficult to estimate for lunar orbits whose orbit plane is close to the earth-moon plane, assuming the use of earth-based observations only. Therefore, the second consideration in the choice of beacon sites is that the beacons should be located to provide information about these elements. The third consideration is that the beacons should be located close enough to the orbit plane to provide adequate tracking periods.

For evaluation of the second consideration, the partial derivatives of the observations with respect to the elements of concern (i.e., $\partial\rho/\partial i$, $\partial\rho/\partial\Omega$, $\partial\dot{\rho}/\partial i$, $\partial\dot{\rho}/\partial\Omega$) can be examined to get some idea of the information content of the observations as a function of the location of the beacons. In general, the larger the partials the greater the quantity of information contained in the corresponding observations. These partial derivatives, developed in appendix A, may be approximated for the orbit considered by the following expressions:

$$\frac{\partial\rho}{\partial i} \approx \frac{rR}{\rho} \sin\theta \sin\phi$$

$$\frac{\partial\rho}{\partial\Omega} \approx \frac{-rR \cos\phi}{\rho} \left[\sin(\lambda' + \theta) \right]$$

$$\frac{\partial \dot{\rho}}{\partial i} \approx \frac{-R \sin \phi}{\rho} \left(\frac{\dot{\rho} r}{\rho} \sin \theta - \sqrt{\frac{\mu}{r}} \cos \theta \right)$$

$$\frac{\partial \dot{\rho}}{\partial \Omega} \approx \frac{-rR \cos \phi}{\rho} \left[\frac{\dot{\rho}}{\rho} \sin(\lambda' + \theta) + \left(\omega_m + \frac{1}{r} \sqrt{\frac{\mu}{r}} \right) \cos(\lambda' + \theta) \right]$$

where

ϕ latitude

λ longitude

θ true anomaly

Ω longitude of the ascending node

$\lambda' = \lambda - \Omega$

From these partial derivatives it can be determined that the maximum information will be obtained about the inclination angle when the beacon is located as far out of the orbit plane as possible. The node partials will be maximum when the beacon is located in the orbit plane ($\phi = 0°$) and 45° from the line of nodes ($\lambda' = 45°$). The beacon is in view of the satellite when $\lambda' = \theta$. Because no information is obtained about the inclination angle when the beacon is located in the plane and very little information about the node angle is lost for small-out-of-plane angles, the beacons should be located out of the orbit plane and at 45° or 90° from the line of nodes. Of course, this last criterion conflicts with the requirements of consideration 3, because as the beacon is moved out of the orbit plane the tracking period is reduced and, consequently, the total information of the observations is reduced since fewer observations can be made. A compromise is necessary and will now be considered.

The time that the beacon is in view is a function of the out-of-plane angle. An expression for the in-view time is derived in appendix B and is given below:

$$t = \frac{P}{\pi} \cos^{-1} \left(\frac{RB}{r \cos \alpha} \right)$$

where

t time beacon is in view of satellite

P period of satellite

RB distance from the center of moon to the beacon

r distance from the center of moon to the satellite

α out-of-plane angle of the beacon with respect to the orbit plane (α is assumed to be equal to the latitude.)

The maximum out-of-plane angle for the beacon to be seen from the orbit considered in this study is approximately 23°. In order to assure three observations per pass (5-min observation intervals), the maximum out-of-plane angle to be considered is 10°.

ANALYSIS AND RESULTS

This study consists of five parts. Part one considers estimating beacon location using earth-based tracking only. In part two the object is to determine what accuracy is required of on-board observations relative to some given earth-based accuracy for such observations to prove beneficial in estimating the state. Part three evaluates the contributions of certain subsidiary parameters. Part four is an evaluation of estimation performance using those beacon locations which had been determined to be best for the particular orbit considered. Part five is concerned with the use of on-board observations as the only source of tracking information.

The results of this study are presented as a series of time histories of the rms errors in the quantities being estimated. The rms error, the ordinate of the figure, is defined as the square root of the appropriate diagonal terms of the covariance matrix; for example, the rms error in position is

$$rmsp = (\sigma_x^2 + \sigma_y^2 + \sigma_z^2)^{1/2}$$

The improvement obtained by the addition of on-board measurements will be given in the text as the percentage improvement over considering earth-based range-rate measurements only; that is,

$$\text{Percent improvement} = \frac{rmsp\left(\begin{array}{c}\text{earth-based}\\\text{range-rate only}\end{array}\right) - rmsp\left(\begin{array}{c}\text{earth-based range rate}\\\text{plus on-board observations}\end{array}\right)}{rmsp(\text{earth-based range-rate only})} \times 100$$

The times when the stations and beacons are in view of the vehicle are indicated by horizontal blocks at the top of figures for all plots given in the report.

Some of the figures in the report have a sufficient number of curves to make their labeling difficult. In order to simplify this as much as possible, the information pertinent to the curves is given in two tables. An example of these tables and an explanation of the symbols are given below.

TABLE 1.- MEASUREMENT ACCURACIES AND INITIAL BEACON ERRORS

Code	Measurement accuracy			Initial beacon errors					
	Earth-based (E)	On-board (OB)		Bcn A (A)			Bcn B (B)		
	$\sigma_{\dot{\rho}}$, m/s	$\sigma_{\dot{\rho}}$, m/s	σ_{ρ}, m	σ_N, m	σ_E, m	σ_D, m	σ_N, m	σ_E, m	σ_D, m
1	0.04	0.3	---	1000	1000	1000	1000	1000	1000
2	---	---	30	---	---	---	100	100	100

TABLE 2.- CONDITIONS CONSIDERED IN RUNS AND SYMBOLS
TO IDENTIFY THE ASSOCIATED CURVES

Symbol	Conditions for the run
□	E
○	E + OB(1) + A(1) + B(1)
◺	E + OB(2) + A(1) + B(1)
◇	E + OB(1) + OB(2) + A(1) + B(1)
△	E + OB(1) + OB(2) + A(1) + B(2)

Table 1 contains the noise figures for the observations and for the various beacons considered. These noise figures, as given in the table, are associated with one of two possible codes. Table 2 gives the symbols used to identify the curve and the various conditions considered in the runs plotted.

The following mnemonics are used in table 2.

E   earth-based observations

OB(I)   on-board observations with noise code I

χ(I)   beacon χ with location error code I

Thus, for example, ◇--E + OB(1) + OB(2) + A(1) + B(1) in table 2 means that the curve designated by the symbol ◇ represents a run that includes earth-based observations, on-board range-rate observations, and on-board range observations of two lunar beacons, A and B, both with location errors of 1000 m in each coordinate.

Beacon Estimation From Earth-Based Measurements

This section considers how accurately the location of the beacon can be estimated using only earth-based range and range-rate observations.

Figures 1(a) and 1(b) show the rms values of beacon location errors (total north, east, and down errors) for beacons located on the front side of the moon and being tracked by three earth-based radars. Figure 1(a) shows results for beacon 1 ($\phi = 0°$, $\lambda = 91.8°$) and 1(b) shows results for beacon 2 ($\phi = 10°$, $\lambda = 45°$). The beacons are tracked for 9 days with both range and range-rate observations taken every 2 hours. The measurement accuracies assumed are $\sigma_\rho = 7.52$ m; $\sigma_{\dot\rho} = 0.00012$ m/s, and the initial beacon errors are 1 km in each coordinate.

Figure 1(a) shows that a significant improvement (from 1 km to 0.18 km) is obtained in the east component of beacon location with the first observation. This improvement occurs because the beacon is located on the limb of the moon as seen from the earth, and therefore, the east component of its position is very nearly colinear with the range observation from the tracking station. Thus, it should be expected that range data would give the most immediate information in this component. As more observations come with time, gradual improvements will be seen in all

components. This is due to the parallax effects (i.e., the beacon will be viewed at slightly different angles from the various stations at the various times).

The total rms error in the knowledge of beacon location $(\sigma_N{}^2 + \sigma_E{}^2 + \sigma_D{}^2)^{1/2}$ is also plotted in figures 1(a) and 1(b), and is seen to be the same for both beacons. This is as expected because the same initial errors and measurement accuracies are assumed. The improvement seen in each coordinate is a function of the beacon location but the total beacon error should be independent of the location.

State Estimation Using On-board Beacon Track and Earth-Based Track

This section considers the question of how accurate the on-board data must be, relative to earth-based data, in order for the use of lunar beacons to be beneficial in the estimation of the position and velocity of a lunar orbiting vehicle. Figure 2 shows a comparison between using earth-based range-rate observations only and using these earth-based observations combined with on-board observations. On-board range and range-rate observations of two beacons are assumed. These beacons are located such that one is on the back of the moon and one on the front and they are approximately 90° apart in longitude. No attempt was made to locate the beacons in the most favorable position for the orbit being considered. The beacon coordinates are given below. In all runs considered, the initial beacon error is assumed to be 1 km in each coordinate unless otherwise stated.

Beacon	Latitude, deg	Longitude, deg
1	0	91.8
2	-10	176
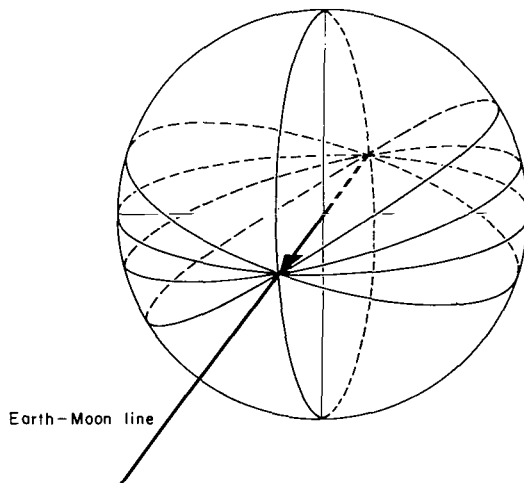
Sketch (b)

The top curve in figure 2 shows the use of earth-based track only $(\sigma_{\dot{\rho}} = 0.04 \text{ m/s})$. After only a short period of tracking, a steady-state situation develops; that is, the position error varies periodically between a maximum which is 36 percent below the initial error to a minimum which is almost an order of magnitude lower than the initial error. Apparently, very little information is obtained from subsequent observations after the initial improvement, which suggests that some portion of the state of the vehicle is poorly observable. The periodicity of the curves in figure 2 is equal to the periodicity of the lunar orbit, a fact which can be explained with the aid of sketch (b). Illustrated in the sketch is a family of orbits, all of whose lines of nodes lie on the earth-moon line. These orbits are virtually indistinguishable when only range-rate data from earth-based stations are used, that is, each produces the same or very similar range-rate

data in spite of a wide variation in the orbit inclination. All the orbits have a pair of common points on the line of nodes. Thus, the position of the vehicle must be best known at these points. On the other hand, the largest variation between orbits occurs 90° from the line of nodes, and at these points the position of the vehicle will be least certain of all points on the orbit.

When the actual orbit being observed does in fact belong to the family illustrated in sketch (b), or is very close to some member of the family, the strong periodic behavior of position estimation error shown in figure 2 will always be observed. For other orbits similar periodicity will often be observed, but with less pronounced differences between the maxima and minima, depending upon how closely the orbit resembles a member of the indistinguishable family.

The second curve from the top in figure 2 shows the case where on-board range and range-rate ($\sigma_\rho = 30$ m; $\sigma_{\dot\rho} = 0.3$ m/s) observations of two lunar beacons are added to the earth-based observations. This addition shows, after three orbits of track, some 45 percent improvement over earth-based observations only. The third curve from the top shows improvement obtained from the addition of on-board track when it is assumed that the location of the front side beacon is known more accurately (to 100 m in each coordinate). This shows, at the maximum uncertainty points, about a 50 percent improvement over earth-based track alone, which is not a really significant improvement over the case with the less accurately located beacon. The reason for this is that, since beacon location is being estimated simultaneously with the vehicle state, the beacon location becomes known nearly as well in the latter case as in the former after a short period of tracking. The advantage of using the more precisely located beacon thus shows up principally in the early part of the tracking. After only about 1 hour of track, there is approximately 19 percent improvement over both the other cases.

The middle group of curves in figure 2 show the results obtained with a more accurate earth-based tracker ($\sigma_{\dot\rho} = 0.002$ m/s). This group of curves again afford a comparison between earth-based only and earth based plus on-board observations. The top curve in this group is for earth-based observations only and this shows a reduction of about 89 percent in the rms error after three orbits of track compared to the 36 percent reduction obtained for the less accurate earth-based measurements. The second curve from the top shows results for the addition of on-board range and range-rate observations with the same accuracies as used in the previous case (i.e., $\sigma_\rho = 30.5$ m; $\sigma_{\dot\rho} = 0.3$ m/s). The addition of on-board observations with these accuracies provides very little improvement (2 percent). The third curve from the top of this group shows results obtained when the on-board observations are assumed to be more accurate than in the previous case ($\sigma_\rho = 4.8$ m; $\sigma_{\dot\rho} = 0.048$ m/s). Here an improvement of approximately 46 percent is obtained after three orbits of track. The next curve down is the same case except that the location of the front side beacon is known to 100 m in each coordinate. There is a 48 percent improvement over earth-based observations only after three orbits of track. Note that the beacon location accuracy does not make as much difference here as it did for less accurate observations.

The bottom group of curves in figure 2 are for runs with extremely accurate earth-based range-rate observations ($\sigma_{\dot\rho} = 0.00012$ m/s). The top curve of the group is for two conditions, (1) earth-based observations only and (2) earth-based observations plus on-board range and range-rate observations with the final accuracies from the cases above ($\sigma_\rho = 4.8$ m; $\sigma_{\dot\rho} = 0.048$ m/s). This shows a couple of orders of magnitude reduction from the initial rms errors in position. The addition of the on-board measurements of this accuracy does not improve the estimation. The next

curve down is for the addition of more accurate on-board measurements ($\sigma_\rho = 1$ m; $\sigma_{\dot\rho} = 0.01$ m/s) and this shows a 30 percent improvement for the use of beacons.

The following conclusions can be reached from the results shown in figure 2.

1. As mentioned previously, some elements of the state of a lunar orbiting vehicle can be only poorly determined when earth-based observations are the only tracking information. However, this condition improves as the accuracy of the tracker increases or on-board measurements are added.

2. Only a modest improvement is achieved by the addition of on-board measurements using beacons at the specified locations. The effect appears to be that such beacon measurements contain roughly the same kind of information as does earth-based tracking, and the result is an effective increase in overall measurement accuracy.

3. The effect of using more accurately located beacons is insignificant. This is probably due to the fact that the system is estimating beacon locations simultaneously and after a short time the location errors are down to about the same level.

4. Although the amount of good done by beacon observations obviously depends upon the relative accuracy of the earth-based and on-board measurements, the on-board measurements need not be nearly as accurate as the earth-based to produce a significant improvement in estimation performance.

The Estimation of Subsidiary Parameters

The subsidiary uncertainties considered in this study are all the unknown parameters, other than vehicle position and velocity, which may significantly influence the observations. These include location uncertainties for both the earth-based stations and the lunar beacons, local clock errors for the earth-based stations and bias errors in the earth-based range-rate data and in the on-board range and range-rate data. In this section the performance of the system in estimating these parameters is shown.

Figures 3(a), (b), and (c) show how the rms uncertainty in the knowledge of earth-based station location is reduced by the use of the observations from earth-based stations. These figures show only the errors for the Woomera station. Range-rate observations were assumed to be taken every 5 minutes when the vehicle was in view of the station. There were 67 observations during a 7-hour interval (7 from Goldstone, 53 from Woomera, and 7 from Johannesburg). The figures show that there is essentially no improvement in the knowledge of station coordinates for the case where the earth-based measurement is least accurate ($\sigma_{\dot\rho} = 0.04$ m/s). They also show very little reduction in latitude errors (5 and 18 percent) but relatively large reduction in height and longitude errors (50 and 94 percent) for the more accurate earth-based observations ($\sigma_{\dot\rho} = 0.002$ m/s and $\sigma_{\dot\rho} = 0.00012$ m/s, respectively).

Figure 4 shows the estimation performance for station clock errors for the three earth-based accuracies. It can be seen that station clock errors do not contribute much to system inaccuracy. Only for extremely accurate earth-based observations ($\sigma_{\dot\rho} = 0.00012$ m/s) is any change (5 percent)

at all noticed. Thus, it can be concluded that time errors of this magnitude (σ_T = 0.0066 s) are not significant and could have been omitted from the analysis.

Figure 5 shows a reduction in range-rate bias error of 22, 79, and 98 percent for the three different earth-based accuracies. The reducing of the errors in the station locations and the range-rate bias amounts to a partial calibration of the tracking system.

Figures 6 to 8 will show errors associated with beacon measurements. Figure 6 shows results for on-board range and range-rate bias errors, while figures 7 and 8 show results for beacon location errors. In each of these figures, three cases are considered, which differ only in the accuracies assumed for the measurements. These cases and their accuracies are as follows:

	Tracking accuracies		
	Earth-based	On-board	
Case	$\sigma_{\dot{\rho}}$, m/s	σ_{ρ}, m	$\sigma_{\dot{\rho}}$, m/s
I	0.04	30	0.3
II	.002	4.8	.04
III	.00012	1.0	.01

Figure 6(a) shows a reduction in the on-board range bias error of 50 percent for case I, 95 percent for case II, and two orders of magnitude for case III. Figure 6(b) shows no improvement in the on-board range-rate bias error for case I, 55 percent improvement for case II, and 90 percent improvement for case III. The quantized appearance of the plots in figure 6(b) is due to the fact that the data were available from the output only in increments of 1 m/s.

Figures 7(a), (b), and (c) are time histories of the rms errors in latitude, longitude, and height, respectively, for beacon 1 ($\phi = 0°$, $\lambda = 91.8°$). The initial location error is assumed to be 1 km in each coordinate. Figure 7(a) shows that only a 10 percent reduction in the latitude error is obtained for case I. Case II gives a reduction of 64 percent and case III has an order-of-magnitude reduction. Figure 7(b) shows significant improvement in knowledge of the longitude of the beacon for all three cases. This improvement ranges from an order of magnitude for case I to two orders of magnitude for case III. Figure 7(c) also shows significant improvement in the knowledge of the height of the beacon for all three cases, ranging from one-and-one-half to approximately three orders of magnitude. The satellite is being tracked from three earth-based stations and the beacon is being observed from on-board the satellite. Since the beacon is directly under the orbit track and the orbit is at a low inclination, the on-board track should provide more information in longitude and height than in latitude. The sharp drops in the estimation error variances occur when the beacon is actually being observed by the satellite. It is also seen that an improvement in estimation of beacon 1 error occurs when beacon 2 is being observed because of the correlation which develops between these errors in the course of processing the data. The track time is noted at the top of the figure.

Figures 8(a), (b), and (c) are the same as 7(a), (b), and (c) but for beacon 2 ($\phi = -10°$, $\lambda = 176°$). Since beacon 2 does not lie directly under the orbit track, more improvement is expected in the latitude error and the height improvement will not be as much as before. Good

15

improvement is still expected in the longitude error. Figure 8(a) shows an 85 percent improvement for case I, 98 percent for case II, and one order of magnitude for case III in latitude estimation. Figure 8(b) shows improvement from one order of magnitude for case I to three orders of magnitude for case III in longitude estimation. Figure 8(c) shows improvement from 85 percent for case I to two-and-a-half orders of magnitude for case III in height estimation. The total rms error in beacon location, that is, $(\sigma_N^2 + \sigma_E^2 + \sigma_D^2)^{1/2}$, is the same for both beacons. This might be expected since the same initial errors and the same measurement accuracy are assumed. However, the result is significant in that it indicates that a beacon need not be in view of the earth in order that its location be determined reliably. In effect, it appears that earth-to-vehicle measurements determine the vehicle trajectory, and then vehicle-to-beacon measurements determine the beacon location.

Estimation Performance Using Optimally Situated Beacons

This section evaluates the contribution of on-board observations of lunar beacons.

Figures 9(a) and 9(b) give the time histories of the rms errors in the position of the vehicle for simultaneous earth-based and on-board observations. The measurement accuracies used for these runs are $\sigma_{\dot\rho} = 0.04$ m/s for the earth-based range-rate and $\sigma_\rho = 30$ m and $\sigma_{\dot\rho} = 0.3$ m/s for on-board range and range-rate, respectively. The beacon locations considered for these runs are those determined to be best for the orbit considered. The beacons and their locations are as follows:

Beacon	Latitude, deg	Longitude, deg
C'	-10	135
A	10	45
B	10	5
B'	-10	185
C	10	315
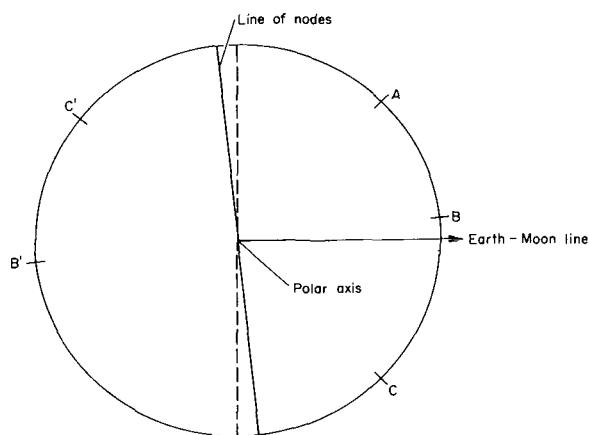
Sketch (c)

Sketch (c) shows the location of the beacons relative to each other, to the line of nodes, and to the earth-moon line. This is looking down on the orbit plane along the North polar axis.

The process of determining these beacon locations was discussed previously in the report. Since the longitude of the node, Ω, is about 95° for the orbit under consideration and the orbit is nearly equatorial, beacon locations A, C, and C' are good for obtaining information about the node angle while beacons B and B' should give good information about the inclination angle.

The curves in figure 9(a) show the performance for combined earth-based on-board

16

tracking for various combinations of beacon locations. The top curve, repeated from figure 2, shows the earth-based only track and is used as the basis of comparison. The second curve from the top shows the addition of on-board tracking of beacons C′ and B to the earth-based track. Beacon C′ is in a favorable location for giving information on the node angle, and beacon B is favorable for giving inclination angle information. This shows an improvement of 47 percent over earth-based only, after three orbits of track.

The nature of this curve indicates that data from such a beacon configuration contains the same type of information as earth-track only data. The next configuration uses beacons A and C′, both of which give maximum information on the node angle; the results are plotted as the third curve from the top and indicate no significant improvement over the previous case. The first configuration (beacons C′ and B) is considered again, but with the B site known more accurately (100 m initial error); the results (fourth curve from the top) show only a slight further improvement (52 percent better than earth-tracking-only data instead of 47 percent). Clearly, better information on the inclination angle is not particularly helpful.

Therefore, two more arrangements were tried which concentrate on gaining the maximum node angle information. The first of these used beacons A and C′ again, but this time with the A site known more accurately (100 m). In this case, a substantial improvement is obtained (77 percent better than earth-tracking only) as shown in the fifth curve from the top. A significant feature of this curve is that the minimum points are shifted markedly from their positions in the earlier runs, in a direction toward the tracking period for beacon A. This suggests the final configuration employed, which uses beacons A and C, both sites being known to 100 m. (Observe that C should give the same amount of node angle information as C′ but since it is on the front rather than the back of the moon, its location can be assumed to be known more accurately.) Both beacons in this configuration are optimally located for node angle information, and both are on the front side where their positions can be estimated more readily from direct earth-based tracking. The results are shown in the lowest curve in figure 9(a), and represents nearly one-order-of-magnitude improvement over earth-tracking only. In addition to this improvement, the periodicity of the error curve has largely disappeared. This disappearance of the error curve periodicity indicates that the information throughout the orbit is approximately the same, or the orbit is more uniformly observable than with any of the earlier configurations. If more accurate observations and better knowledge of the beacon locations are assumed, it is possible that some periodicity might return. In other words, the specific configuration and set of accuracies assumed here appears to be optimal for obtaining uniform observability of the orbit in the tracking period assumed.

In the preceding runs, combined range and range-rate measurements have been assumed for the on-board system. Considerations as to the practicality or economics of implementing both types of measurements in a real system are beyond the scope of this report. However, it is possible to answer some questions as to the relative usefulness of the two types in orbit estimation. The use of on-board range or on-board range-rate measurements with earth-based range-rate measurements is evaluated in the last beacon configuration given (i.e., beacons A and C, both known to 100 m). Figure 9(b) gives the rms error time histories for these cases. The top curve in figure 9(b), which corresponds to the range-rate case, shows an 83 percent improvement over the earth-based-only measurements. The bottom curve is for two cases, range only and the range plus range-rate cases. This curve, identical to the bottom curve in figure 9(a), shows an order of magnitude reduction from the earth-based-only case. It can be concluded from this figure that the on-board range and range-rate measurements give the same kind of information. Thus, in designing a real system both

17

types of measurements need not be used. For the measurement errors assumed, more information is obtained from the range measurements. In fact, as indicated by the lower curve, if on-board range observations are available, no information is obtained by the addition of the on-board range-rate observations.

State Estimation Using On-Board Measurements Only

This section evaluates the use of on-board only measurements of a lunar beacon for state estimation.

Figure 10(a) shows the rms error in position for on-board-only observations of two lunar beacons. The results of these runs will be compared with runs using earth-based-only track ($\sigma_{\dot{\rho}}$ = 0.04 m/s). These earth-based only track results, shown as the top curve in figure 9(a), assume accuracies of σ_ρ = 30 m; $\sigma_{\dot{\rho}}$ = 0.3 m/s. The top two curves in the figure are for cases where beacons A and C' and beacons C' and B' are observed. In both cases there is a 1-km initial error assumed in each beacon component. The results are almost identical, each showing a reduction of approximately 50 percent in the initial error after 7 hours of track. The maximum errors in these curves are slightly less than the maximum error for the cases using earth-based-only track. However, the error in these cases is fairly constant for the whole orbit whereas with the earth-based data, the error in the state is much smaller in some parts of the orbit.

The two middle curves are for the same two cases as the two top curves except that beacon C' is assumed known to 100 m in each coordinate. These cases give slightly better results than earth-based-only data. The bottom curve considers beacons A and C, both known to 100 m in each coordinate. This case shows approximately 75 percent improvement over the earth-based-only case. Since no measurements are available when the satellite is behind the moon, the rms errors increases slightly in this part of the orbit. This figure shows that as is to be expected on-board-only observations of lunar beacons would prove adequate in state estimation, provided that the beacon locations are known accurately enough.

Figure 10(b) gives the rms time histories for cases considering either on-board range or on-board range-rate measurements only. These results are similar to results shown in figure 9(b). Again, for the measurement noises assumed, range observations give more information, but in this case the addition of the range-rate measurements does provide some improvement (7 percent). As noted before, the observations give the same type of information and the availability of both ranges and range-rate observations offer no real advantage.

CONCLUSIONS

The rms error in beacon location can be reduced significantly (from 1.73 km initial error to 0.16 km after 9 hours of track) using earth-based-only measurements (with a 2-hour observation interval) from three earth-based stations (Goldstone, Woomera, and Johannesburg). Both range (σ_ρ = 7.52 m) and range-rate ($\sigma_{\dot{\rho}}$ = 0.00012 m/s) observations were considered.

18

The value of lunar beacon observations is a function of the relative accuracy of the on-board and earth-based measurements. Significant improvement is obtained with on-board measurements (σ_ρ = 30 m; $\sigma_{\dot\rho}$ = 0.3 m/s) much less accurate than the earth-based measurements ($\sigma_{\dot\rho}$ = 0.04 m/s). The improvement is also dependent on the knowledge of the beacon location and the location of the beacon along the orbit track. This study has shown that when the beacons are located to provide information about elements difficult to estimate from earth-based observations, improvements as high as 90 percent are obtained over estimates obtained from earth-based track only. When no attempt is made to locate the beacons in this manner, improvements as high as 50 percent are obtained. These maximum improvements noted above were for cases where the beacons were assumed to be known to 100 m in each coordinate.

The knowledge of subsidiary errors in general do not have much effect when the least accurate earth-based measurements ($\sigma_{\dot\rho}$ = 0.04 m/s) are used. The earth-based station location errors are reduced very little by the use of these measurements. However, considerable improvement is obtained in these estimates as the earth-based measurements become more accurate. Radar timing errors are not significant for any of the accuracies assumed. Significant improvements in the knowledge of range-rate measurement biases is obtained with the more accurate earth-based measurements. Likewise, both on-board range and range-rate bias errors are improved significantly when the more accurate measurements are considered.
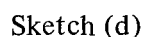
The use of on-board track as the only source of data proved adequate. For the cases where beacon errors were 1 km in each coordinate, the maximum rms errors were about the same as for earth-based-only track. When the front side beacon was assumed to be known more accurately (100 m in each coordinate), slightly better results were obtained from the on-board track only than for earth-based-only track. These cases considered the least accurate measurements for both on-board (σ_ρ = 30 m; $\sigma_{\dot\rho}$ = 0.3 m/s) and earth-based measurements ($\sigma_{\dot\rho}$ = 0.04 m/s).

On-board range and range-rate observations give the same kind of information. For the accuracies assumed for the on-board measurements, range measurements provide more information than range-rate measurements. If the range measurements are available, there is no advantage to including the range-rate measurements.

Ames Research Center
National Aeronautics and Space Administration
Moffett Field, Calif., 94035, May 5, 1970

19

APPENDIX A

THE PARTIAL DERIVATIVES OF RANGE AND RANGE-RATE OBSERVATIONS
WITH RESPECT TO THE INCLINATION ANGLE AND THE
LONGITUDE OF THE NODE ANGLE

The inclination angle and the longitude of the node angle are two quantities that are difficult to estimate for the orbit considered in this report if earth-based-only measurements are available. On-board observations of lunar beacons provide more information about these elements. Since, in general, the larger the partial derivative ($\partial\rho/\partial i$, $\partial\rho/\partial\Omega$, $\partial\dot{\rho}/\partial i$, $\partial\dot{\rho}/\partial\Omega$) the more information contained in the observation, it is advantageous to use beacon locations that maximize these partial derivative expressions. These expressions are derived in this appendix.

From sketch (d) the following relationships can be seen in the x_1, y_1, z_1 frame.

$$\overline{RB} = RB \begin{pmatrix} \cos\phi \\ 0 \\ \sin\phi \end{pmatrix} \qquad \bar{r} = r \begin{pmatrix} l_1 \\ m_1 \\ n_1 \end{pmatrix}$$

Sketch (d)

where

$\left.\begin{array}{l} x_1, y_1, \\ z_1 \end{array}\right\}$ a moon-fixed reference frame

x_1 lies in the lunar equator through the beacon's meridian

z_1 is normal to the lunar equator and is positive in the northern hemisphere

y_1 forms a right-handed system with x_1 and z_1

x,y,z an inertial, selenocentric, rectangular coordinate system

20

x   is positive in the direction of the mean vernal equinox of 1950.0

z   is normal to the mean equator of 1950.0 and is positive in the northern hemisphere

y   forms a right-handed system with x and z

$$l_1 = \cos \theta \cos \lambda' + \sin \theta \cos i \sin \lambda'$$

$$l_2 = -\sin \theta \cos \lambda' + \cos \theta \cos i \sin \lambda'$$

$$m_1 = -\cos \theta \sin \lambda' + \sin \theta \cos i \cos \lambda'$$

$$m_2 = \sin \theta \sin \lambda' + \cos \theta \cos i \cos \lambda'$$

$$n_1 = \sin \theta \sin i$$

$$n_2 = \cos \theta \sin i$$

Hence,

$$\bar{\rho} = \overline{RB} - \bar{r} = \begin{pmatrix} RB \cos \phi - r l_1 \\ -r m_1 \\ RB \sin \phi - r n_1 \end{pmatrix}$$

and

$$\rho = (\bar{\rho} \cdot \bar{\rho})^{1/2} = [RB \cos \phi - r l_1)^2 + (r m_1)^2 + (RB \sin \phi - r n_1)^2]^{1/2}$$

To obtain $\dot{\rho}$, note that λ_0, ω_m, ϕ, Ω, and i are constants.

$$\lambda' = \lambda - \Omega$$

$$\lambda = \lambda_0 + \omega_m \Delta t$$

$$\dot{\rho} = \frac{1}{\rho} [r\dot{r} - RB \cos \phi(\dot{r} l_1 + r\dot{l}_1) - RB \sin \phi(\dot{r} n_1 + r\dot{n}_1)]$$

but

$$\dot{l}_1 = l_2 \dot{\theta} + m_1 \omega_m$$

$$\dot{n}_1 = n_2 \dot{\theta}$$

Therefore,

$$\dot{\rho} = \frac{1}{\rho} \left[r\dot{r} - RB \cos \phi (\dot{r}l_1 + r\dot{\theta}l_2 + r\omega_m m_1) - RB \sin \phi (\dot{r}n_1 + r\dot{\theta}n_2) \right]$$

Thus, the partial derivatives of interest $(\partial\rho/\partial i, \partial\rho/\partial\Omega, \partial\dot{\rho}/\partial i, \partial\dot{\rho}/\partial\Omega)$ are as follows:

$$\frac{\partial\rho}{\partial i} = \frac{rRB \sin \theta}{\rho} (\sin i \sin \lambda' \cos \phi - \sin \phi \cos i)$$

$$\frac{\partial\rho}{\partial\Omega} = -\frac{rRB \cos \phi}{\rho} (\cos \theta \sin \lambda' - \sin \theta \cos i \cos \lambda')$$

$$\frac{\partial\dot{\rho}}{\partial i} = -\frac{1}{\rho} \left\{ \dot{\rho} \frac{\partial\rho}{\partial i} - \frac{RB}{r} \sqrt{\mu a} \left[(E - M)\sin \theta + \sqrt{1 - e^2} \cos \theta \right] (\cos \phi \sin i \sin \lambda' \right.$$

$$\left. - \sin \phi \cos i) - RBr\omega_m \cos \phi \cos \lambda' n_1 \right\}$$

$$\frac{\partial\dot{\rho}}{\partial\Omega} = -\frac{1}{\rho} \left\{ \dot{\rho} \frac{\partial\rho}{\partial\Omega} + RBr\omega_m \cos \phi l_1 - \frac{RB}{r} \sqrt{\mu a} \cos \phi \left[(E - M)m_1 + \sqrt{1 - e^2} m_2 \right] \right\}$$

where

$$\dot{r} = ae\dot{E} \sin E \rightarrow M = E - e \sin E \rightarrow \dot{E} = 1/r \sqrt{\mu/a} \rightarrow \dot{r} = \sqrt{\mu a}/r(E - M)$$

$$\dot{\theta}^2 r^4 = a\mu(1 - e^2) \rightarrow \dot{\theta}r = \sqrt{\mu a} \sqrt{1 - e^2}/r$$

If these partials are evaluated for the case of interest, that is, $a \approx r$, $e \approx 0$, $i \approx 180°$, they can be approximated by

$$\frac{\partial\rho}{\partial i} \approx \frac{rRB \sin \theta \sin \phi}{\rho}$$

$$\frac{\partial\rho}{\partial\Omega} \approx \frac{-rRB \cos \phi \sin(\lambda' + \theta)}{\rho}$$

$$\frac{\partial\dot{\rho}}{\partial i} \approx \frac{-RB}{\rho} \sin \phi \left(\frac{\dot{\rho}r \sin \theta}{\rho} - \sqrt{\frac{\mu}{r}} \cos \theta \right)$$

$$\frac{\partial\dot{\rho}}{\partial\Omega} \approx \frac{-rRB \cos \phi}{\rho} \left[\frac{\dot{\rho} \sin(\lambda' + \theta)}{\rho} + \left(\omega_m + \frac{1}{r} \sqrt{\frac{\mu}{r}} \right) \cos(\lambda' + \theta) \right]$$

APPENDIX B

TIME THAT THE BEACON IS IN VIEW AS A FUNCTION OF

THE OUT-OF-ORBIT PLANE ANGLE

The time that a beacon is in view of a space vehicle is a function of the altitude of the vehicle and the angular displacement of the orbit plane from the beacon. In this study the altitude of the vehicle is fixed and it has been shown in the report that it is advantageous to locate the beacon out of the orbit plane. Therefore, in this appendix an expression is developed to determine the time that the beacon is in view as a function of the out-of-orbit plane angle.
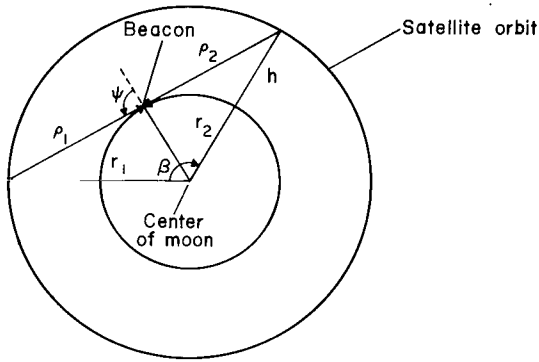
Sketch (e)

First consider the case where the beacon lies within the orbit plane. From sketch (e) it can be seen that ψ, the angle between RB and ρ_i, will be equal to 90° when the beacon comes into view (ρ_1) or goes out of view (ρ_2) of the satellite. This angle varies from +90° to -90° as the satellite passes over the beacon. The angle β, which is a measure of how long the beacon is observed, can be computed as follows:

$$\cos \beta/2 = RB/r_1 = RB/(RB + h)$$
$$\beta = 2 \cos^{-1}[RB/(RB + h)]$$

Since the orbit being considered is essentially circular, then

$$t/P = \beta/2\pi \rightarrow t = (P/\pi)\cos^{-1}[RB/(RB + h)]$$

where

t   time the beacon is in view of the satellite

P   period of satellite orbit

β angle measured in the orbit plane between r_1 and r_2

r_1 distance from the center of moon to satellite at time that beacon comes in view of satellite

r_2 distance from the center of moon to satellite at time that beacon goes out of view of satellite

RB   distance from the center of moon to beacon

23

h   altitude of satellite

ψ angle between RB and ρ_i

ρ_i range from satellite to beacon; i = 1 when beacon comes into view; i = 2 when beacon goes out of view

Now consider the case where the beacon is located out of the orbit plane. From sketch (f) it can be seen again that ψ, the angle between RB and ρ_i, will be equal to 90° when the beacon comes into view (ρ_1) or goes out of view (ρ_2) of the satellite. These two ranges, ρ_1 and ρ_2, define a plane that is perpendicular to RB. As the beacon is moved farther from the orbit plane (a is increased), the plane formed by ρ_1 and ρ_2 is rotated such that it intersects a smaller arc of the orbit plane until eventually it does not intersect the orbit plane. This arc of the orbit plane that is intersected is the part of the orbit that is in view of the beacon. The equation to determine time in view as a function of the out-of-plane angle is determined as follows:
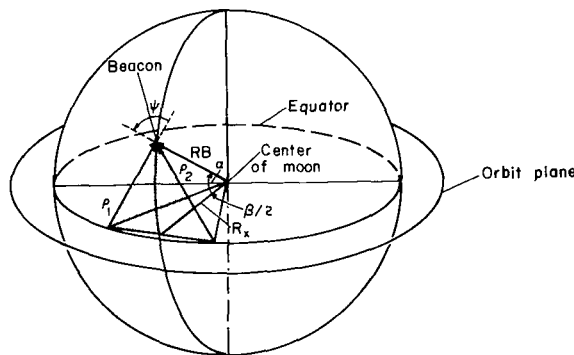
$$R_x = \frac{RB}{\cos \alpha}$$

$$\cos \frac{\beta}{2} = \frac{R_x}{r_2} = \frac{RB}{r_2 \cos \alpha}$$

$$t = \frac{P}{\pi} \cos^{-1} \frac{RB}{r_2 \cos \alpha}$$

where

α out-of-orbit plane angle of the beacon

R_x projection of RB in the orbit plane

Sketch (f)

REFERENCES

1. Smith, Gerald L.; Schmidt, Stanley F.; and McGee, Leonard A.: Application of Statistical Filter Theory to the Optimal Estimation of Position and Velocity On Board a Circumlunar Vehicle. NASA TR R-135, 1962.

2. McLean, John D.; Schmidt, Stanley F.; and McGee, Leonard A.: Optimal Filtering and Linear Prediction Applied to a Midcourse Navigation System for the Circumlunar Mission. NASA TN D-1208, 1962.

3. Smith, Gerald L.: Secondary Errors and Off-Design Conditions in Optimal Estimation of Space Vehicle Trajectories. NASA TN D-2129, 1964.

4. McLean, John D.: Evaluation of a New Method of Integrating the Orbital Equations of Motion for Use in Space Navigation. NASA TN D-3624, 1966.

5. Carson, Thomas M.: Lunar Beacons: A Preliminary Look at Their Position Estimation and Their Use in Lunar Orbit Estimation. NASA TM X-1529, 1968.

6. Compton, Harold R.: A Study of the Accuracy of Estimating the Orbital Elements of a Lunar Satellite by Using Range and Range-Rate Measurements. NASA TN D-3140, 1966.
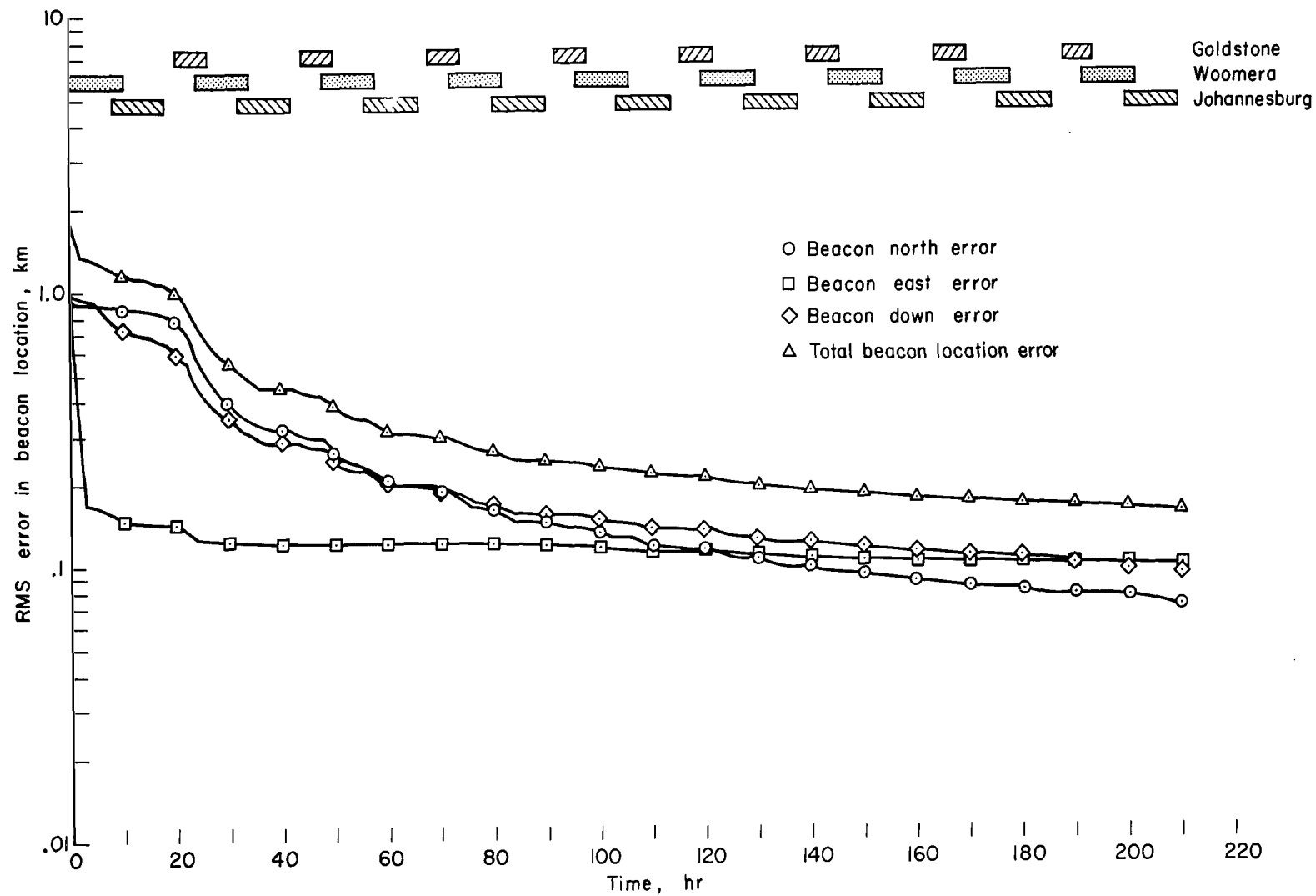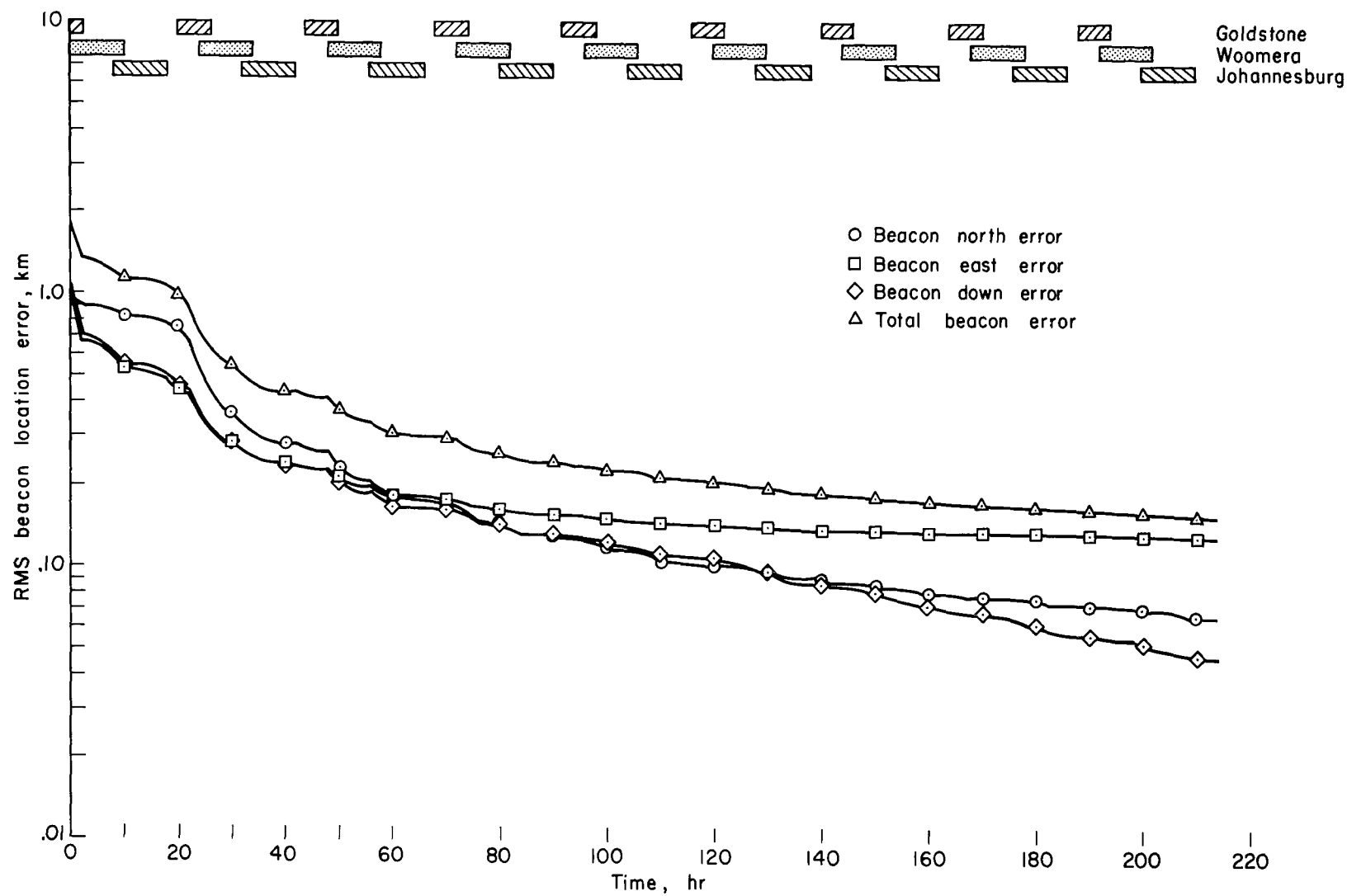
(a) Beacon 1 ($\phi = 0°$, $\lambda = 91.8°$).

Figure 1.- Improvement in estimate of beacon locations using earth-based range and range-rate measurements.

(b) Beacon 2 ($\phi = 10°$, $\lambda = 45°$).

Figure 1.- Concluded.

Code	Measurement Accuracy			Initial Beacon Location Errors					
	Earth-based (E)	On-board (OB)		Beacon 1 (B1)			Beacon 2 (B2)		
	$\sigma_{\dot{\rho}}$ (m/s)	$\sigma_{\dot{\rho}}$ (m/s)	σ_{ρ} (m)	σ_N (m)	σ_E (m)	σ_D (m)	σ_N (m)	σ_E (m)	σ_D (m)
1	.04	.3	30	1000	1000	1000	1000	1000	1000
2	.002	.048	4.8	100	100	100	1000	1000	1000
3	.00012	.01	1						

Goldstone
Woomera
Johannesburg
Beacon 1
Beacon 2

Conditions for run

○ E (1)

□ E (1) + OB (1) + B1 (1) + B2 (1)

◇ E (1) + OB (1) + B1 (2) + B2 (1)

◇ E (2)

△ E (2) + OB (1) + B1 (1) + B2 (1)

◮ E (2) + OB (2) + B1 (1) + B2 (1)

◊ E (2) + OB (2) + B1 (2) + B2 (1)

◮ E (3)

◖ E (3) + OB (2) + B1 (1) + B2 (1)

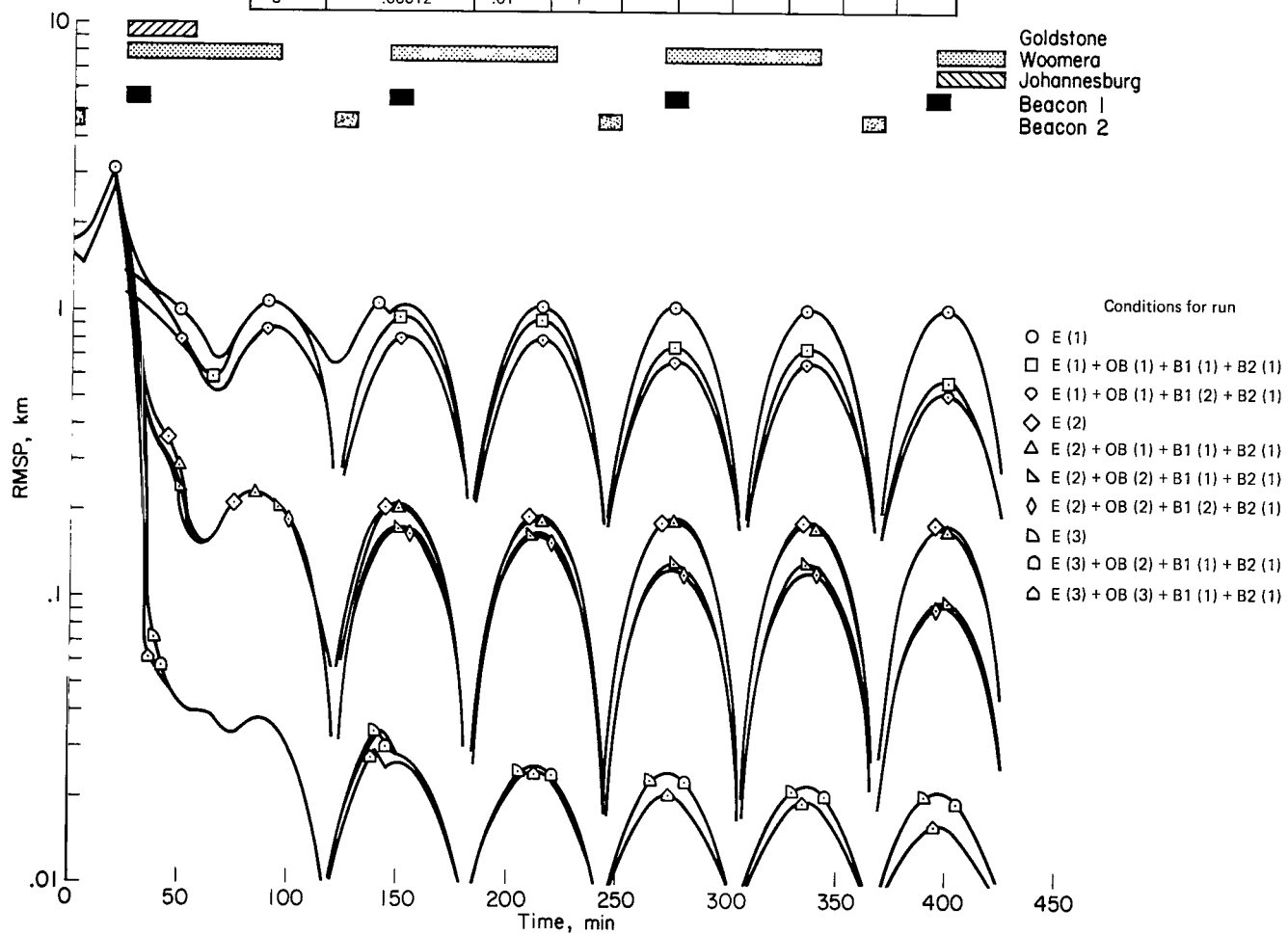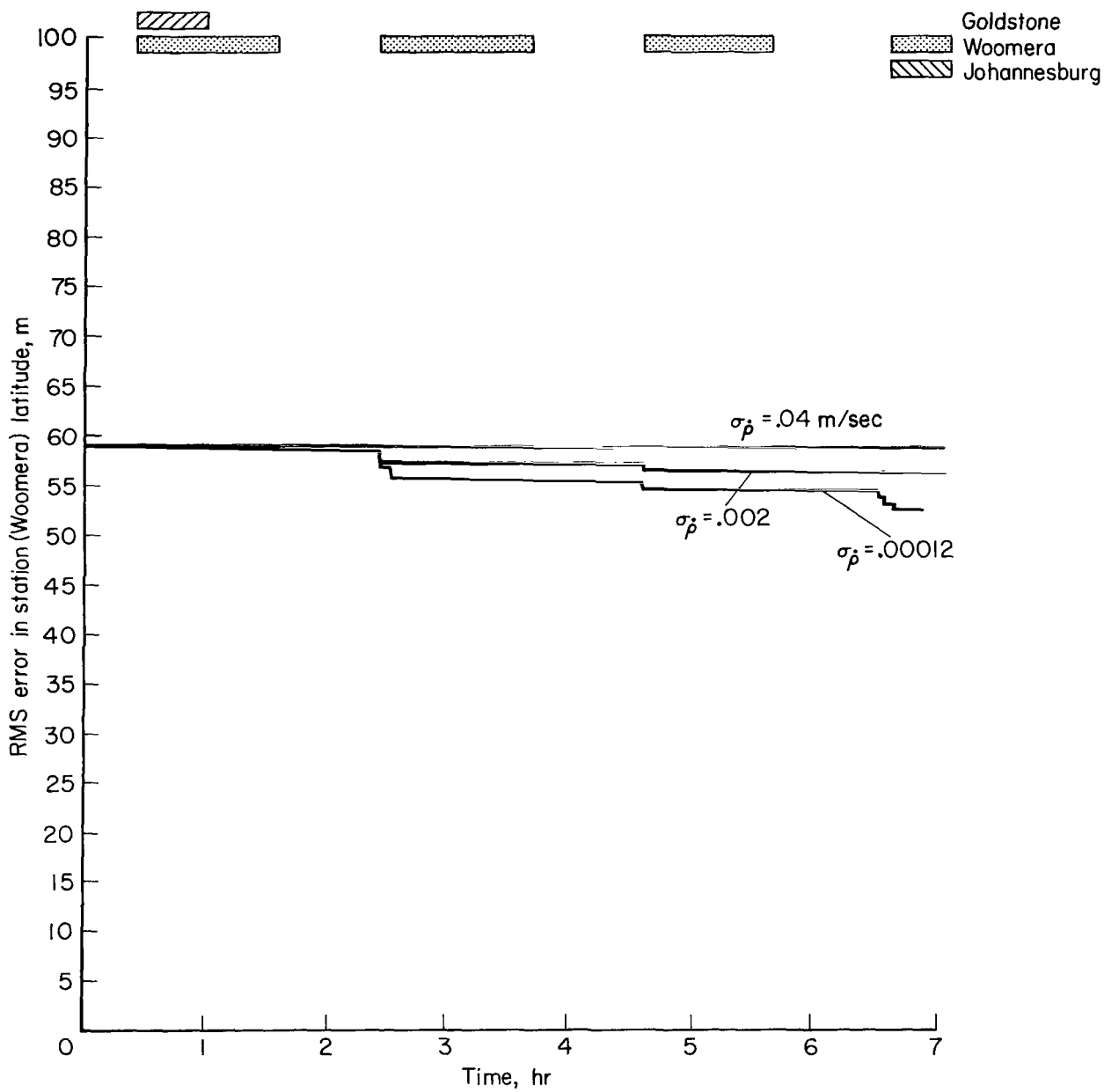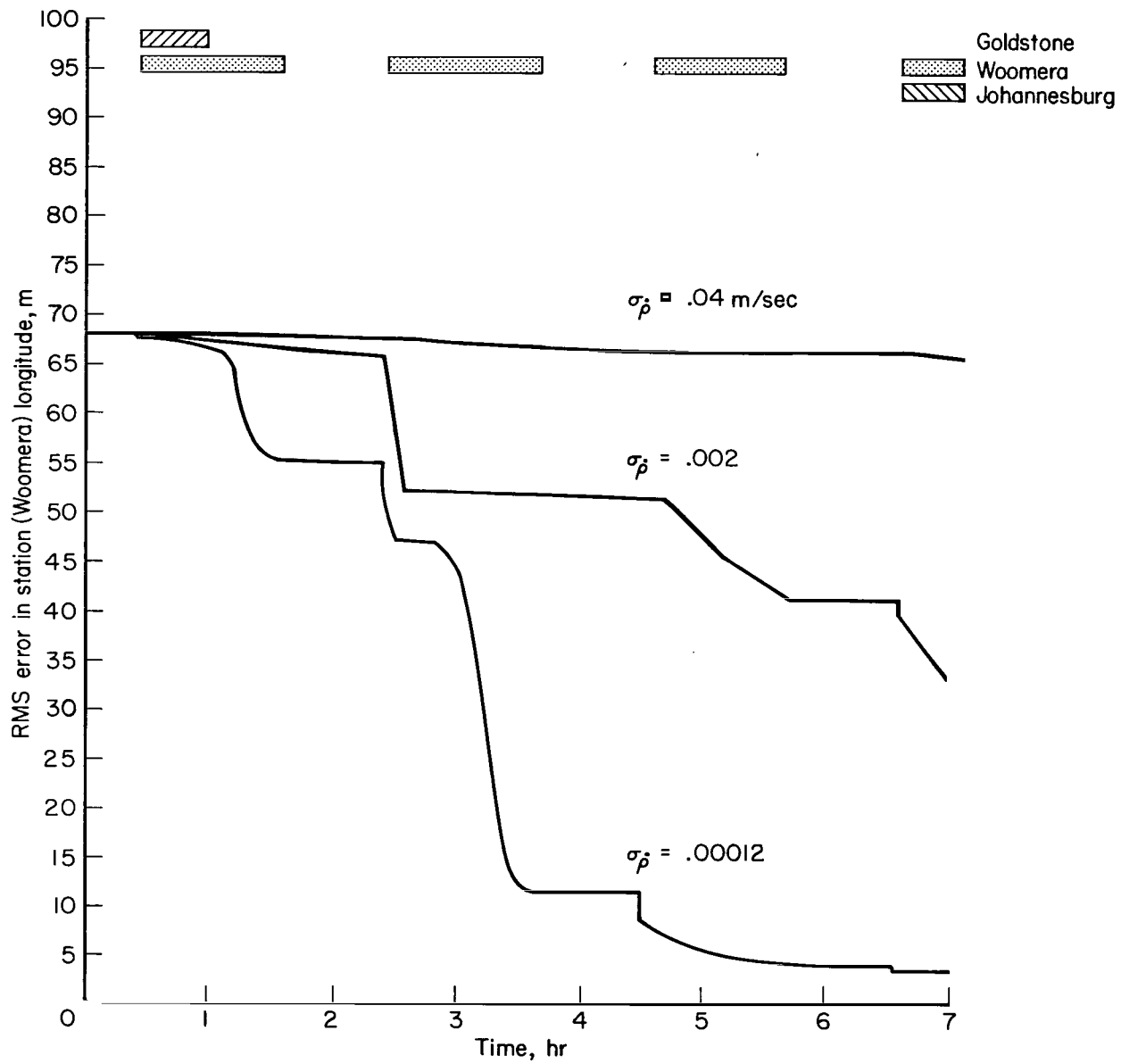△ E (3) + OB (3) + B1 (1) + B2 (1)

RMSP, km

Time, min

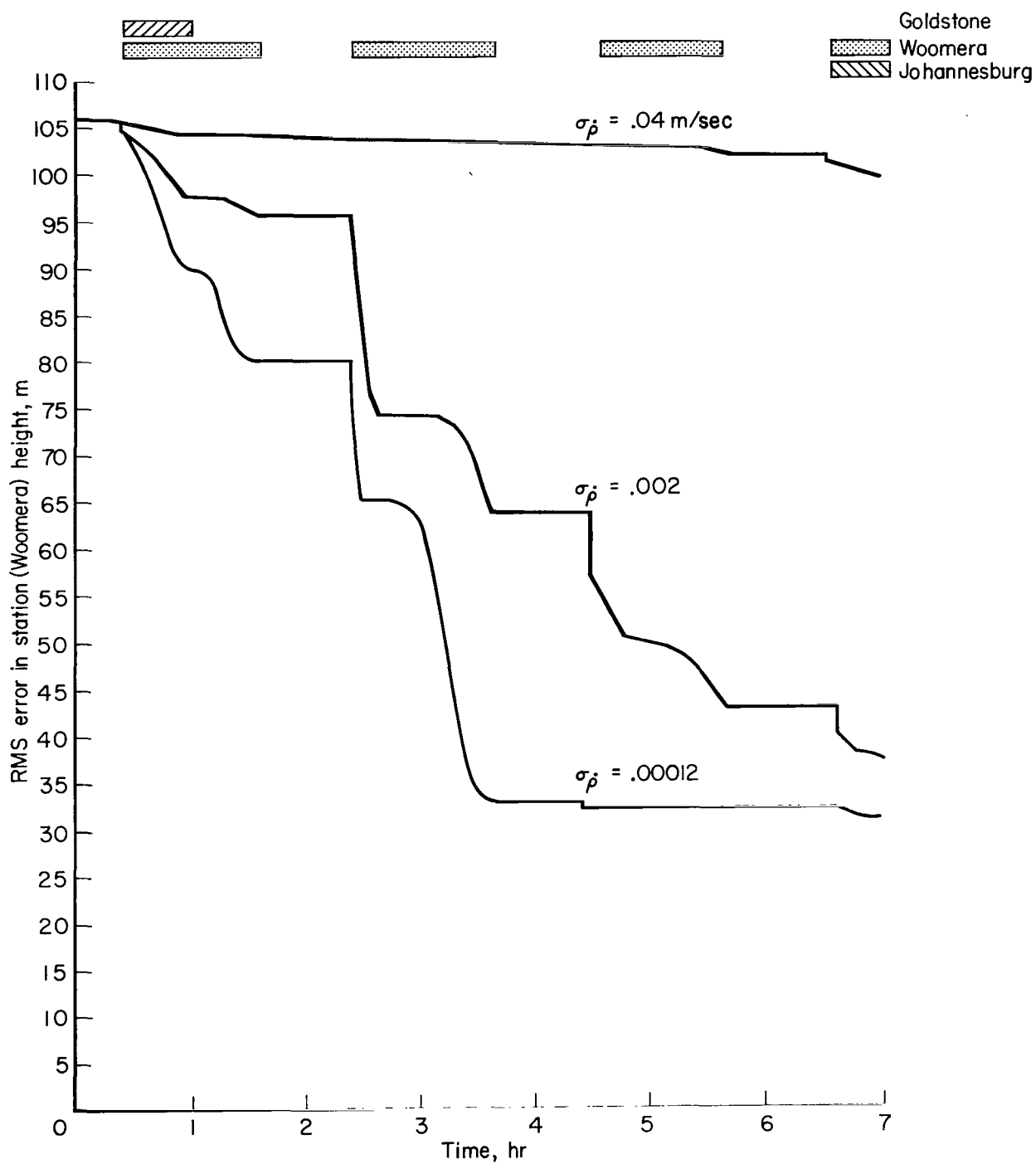Figure 2.- Position estimation error for different measurement accuracies.

(a) Latitude improvement.

Figure 3.- Estimation of error in station coordinates from earth-based measurements.

(b) Longitude improvement.

Figure 3.- Continued.
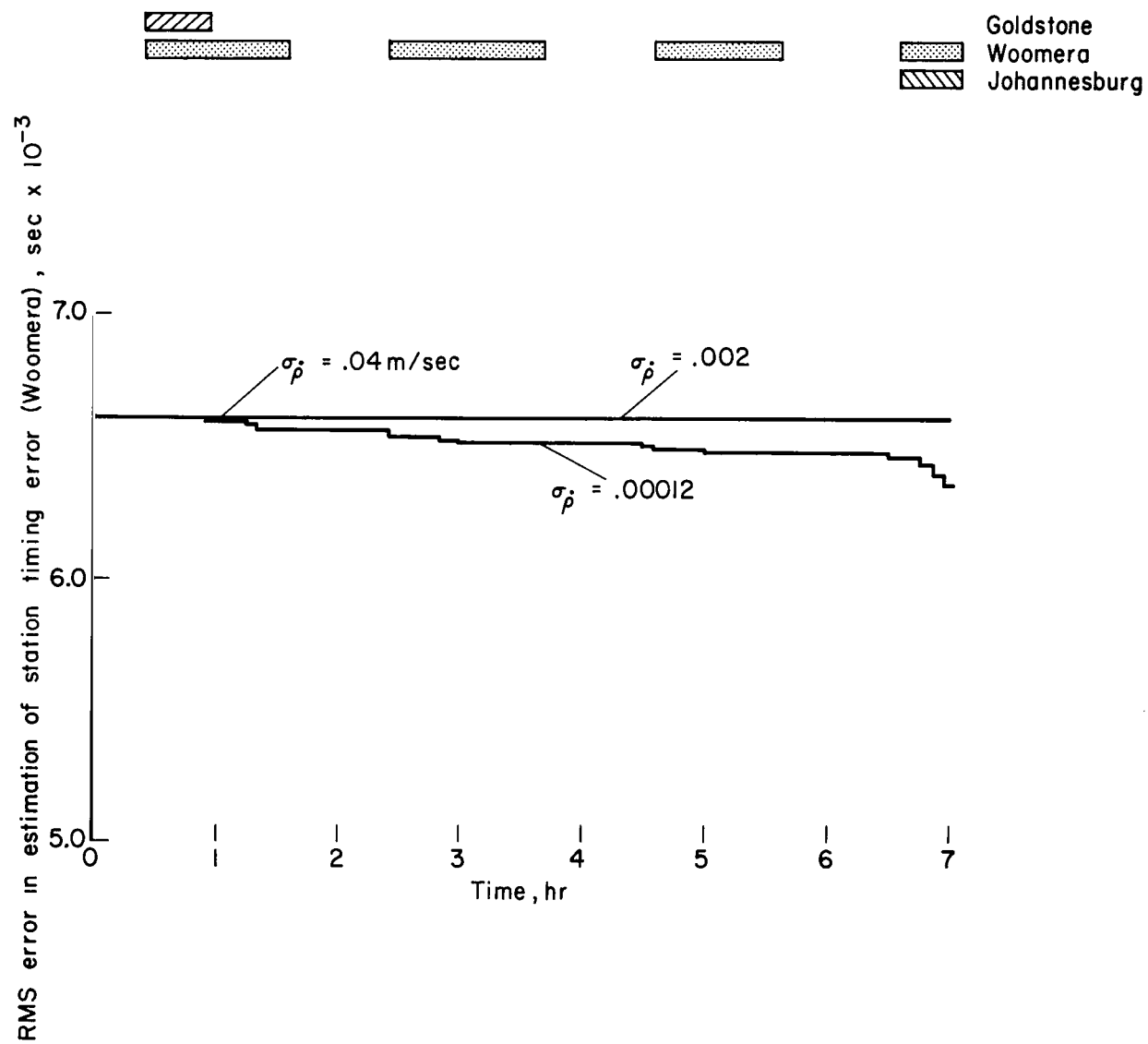
(c) Height improvement.

Figure 3.- Concluded.

Figure 4.- Estimation of radar station timing errors.
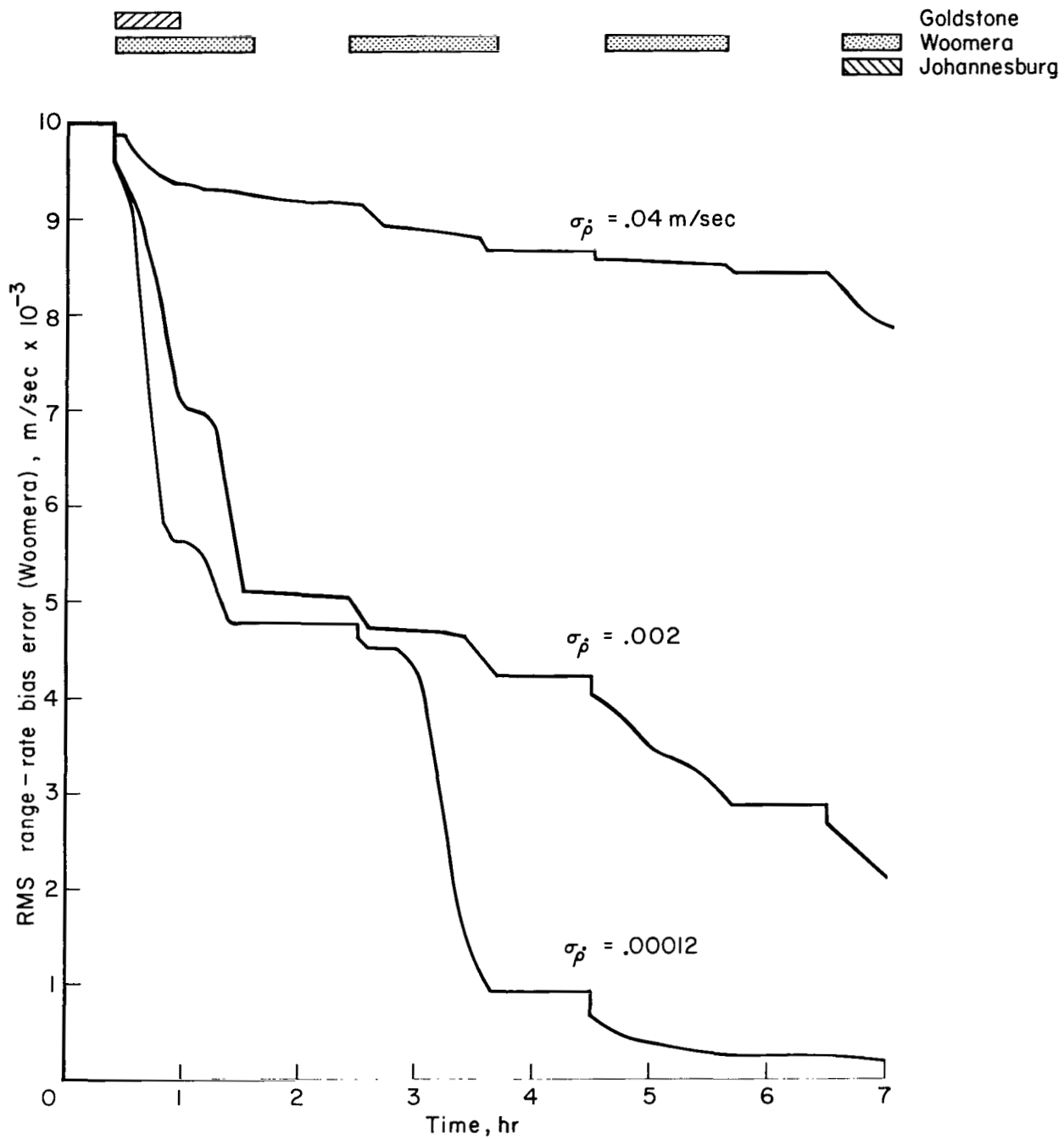
Figure 5.- Estimation of earth-based range-rate bias errors.
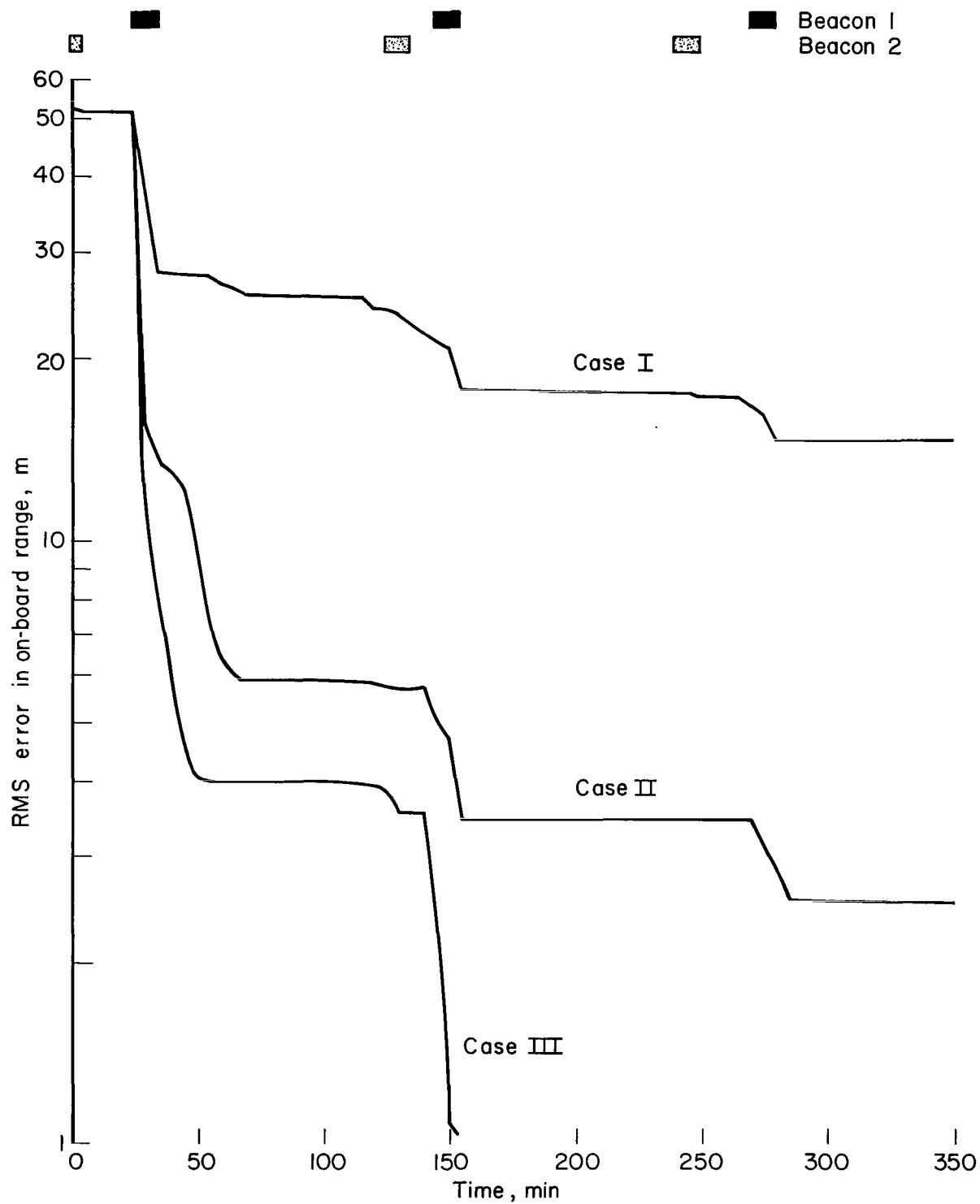
(a) Range bias.

Figure 6.- Estimation of on-board bias errors.
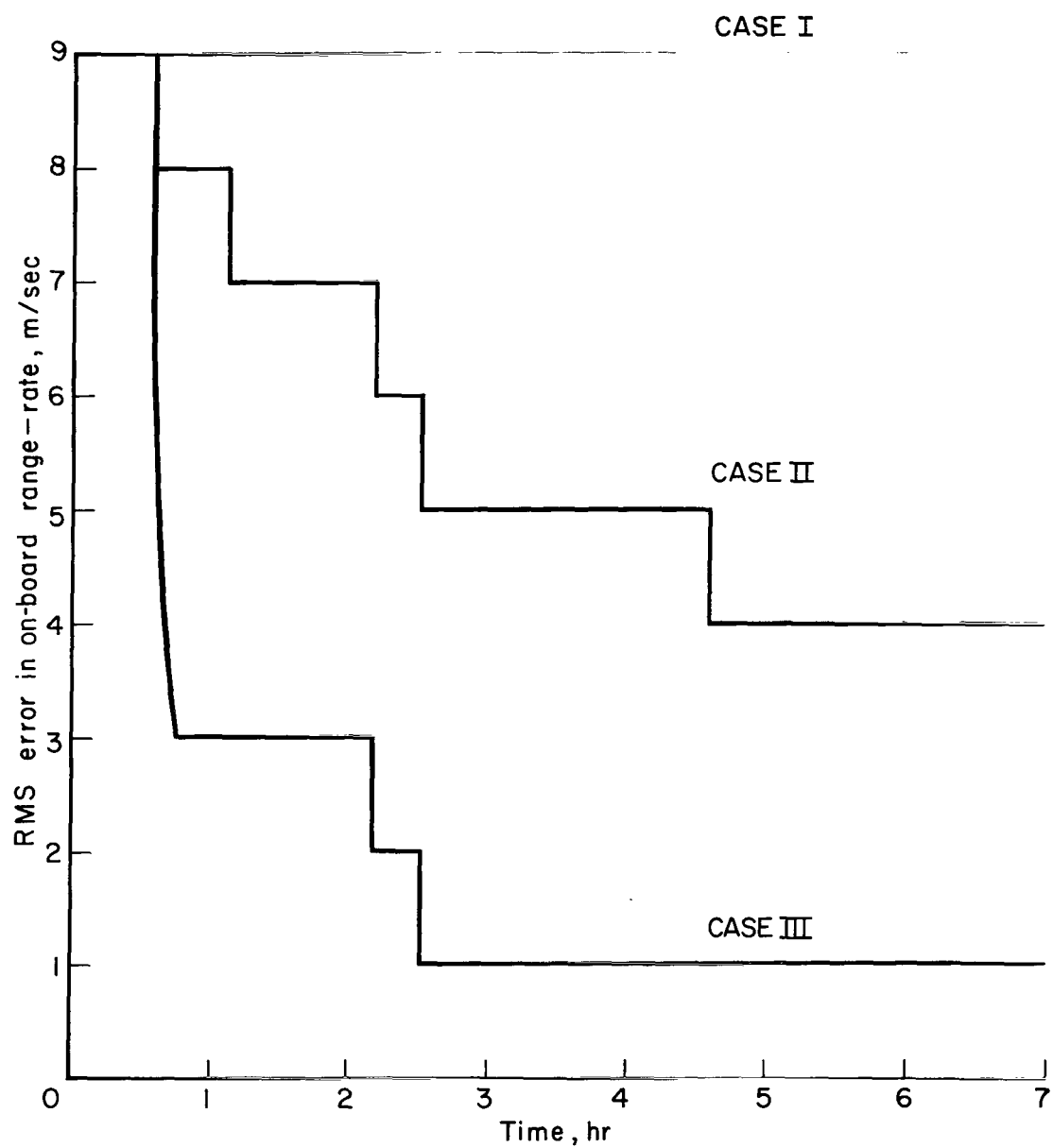
(b) Range-rate bias.

Figure 6.- Concluded.
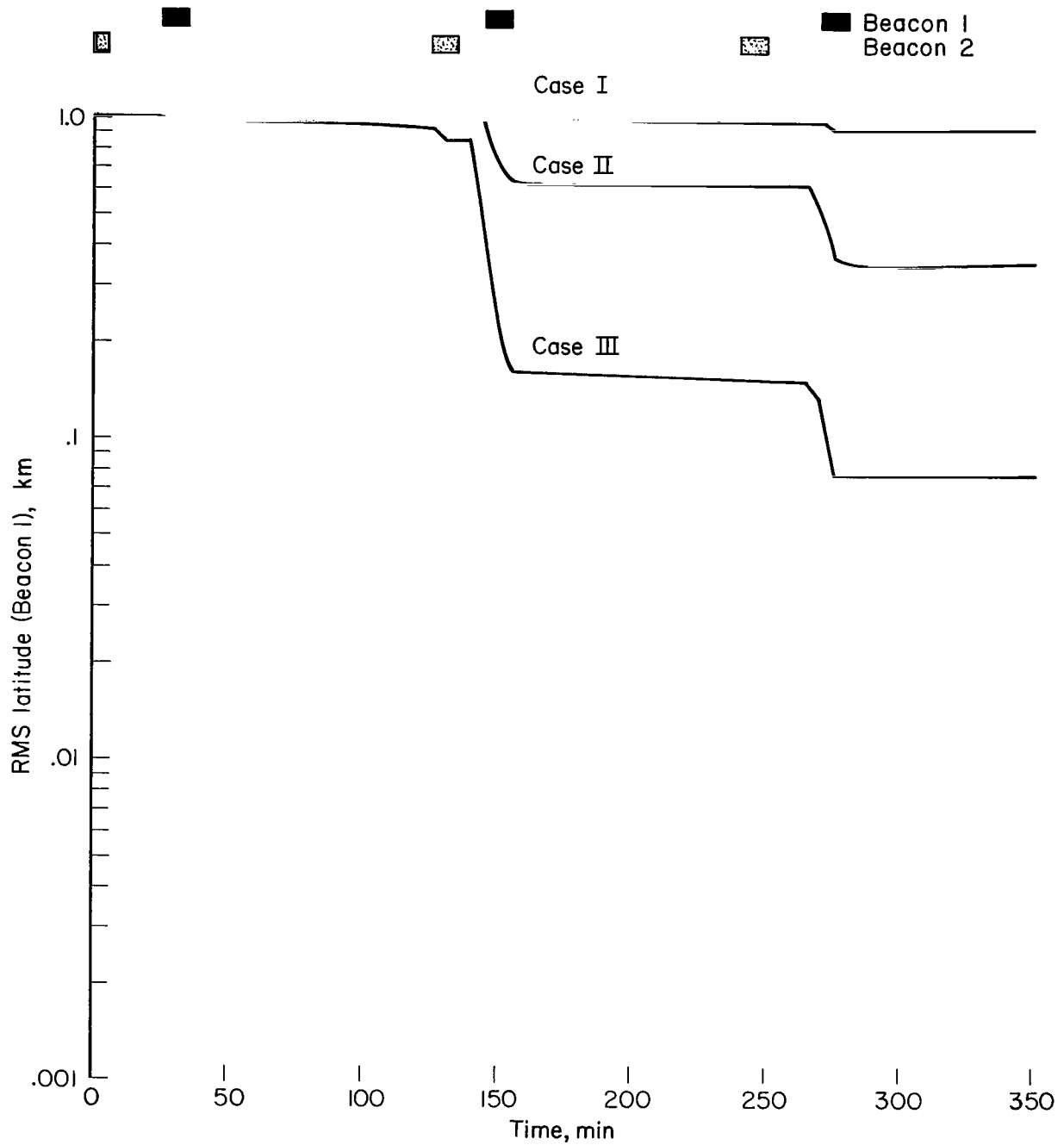
(a) Latitude improvement.

Figure 7.- Improvement in estimate of beacon locations using earth and on-board measurements.

(b) Longitude improvement.

Figure 7.- Continued.

(c) Height improvement.

Figure 7.- Concluded.
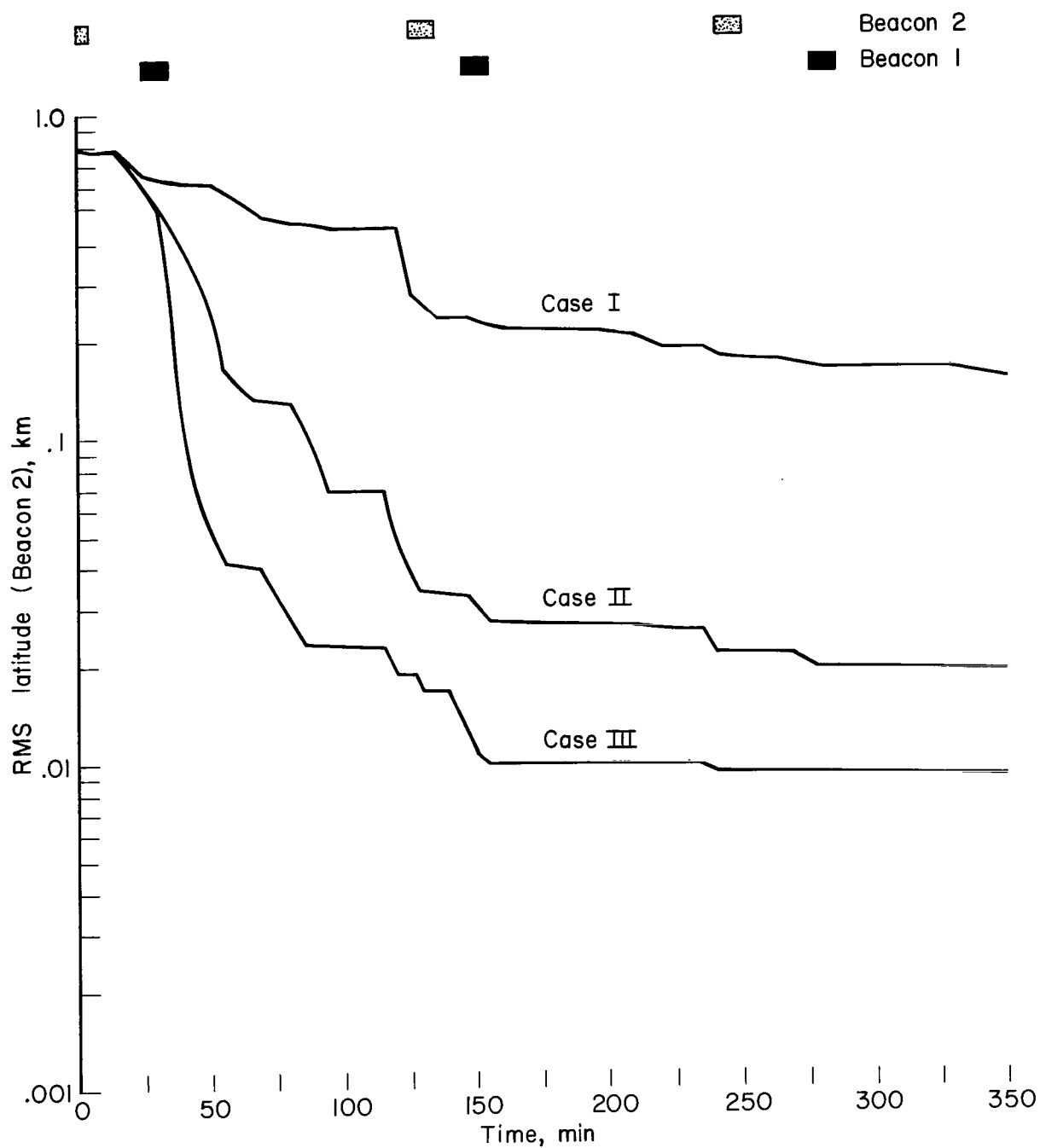
(a) Latitude improvement.

Figure 8.- Improvement in estimate of beacon location using earth and on-board measurements.
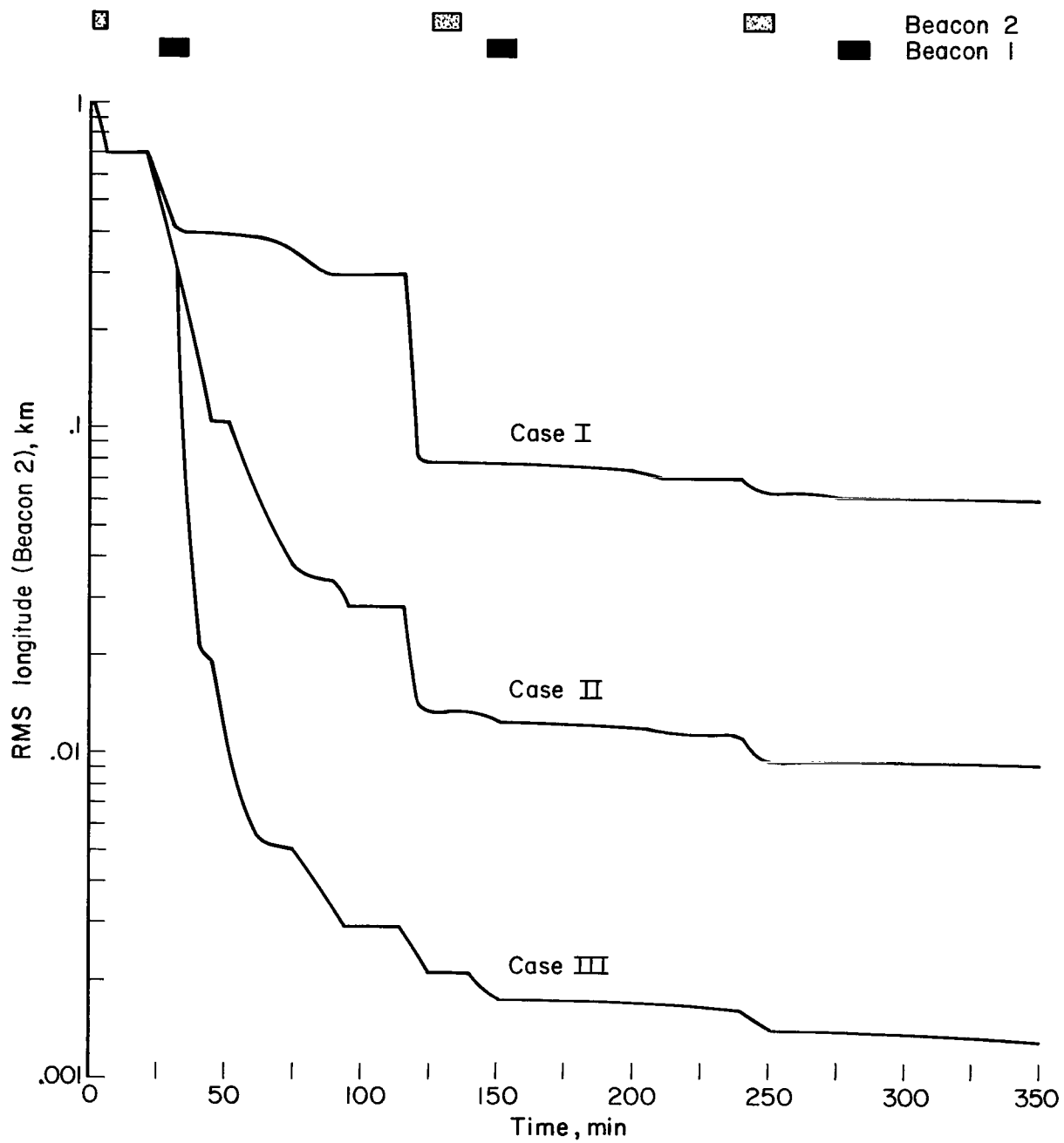
(b) Longitude improvement.

Figure 8.- Continued.
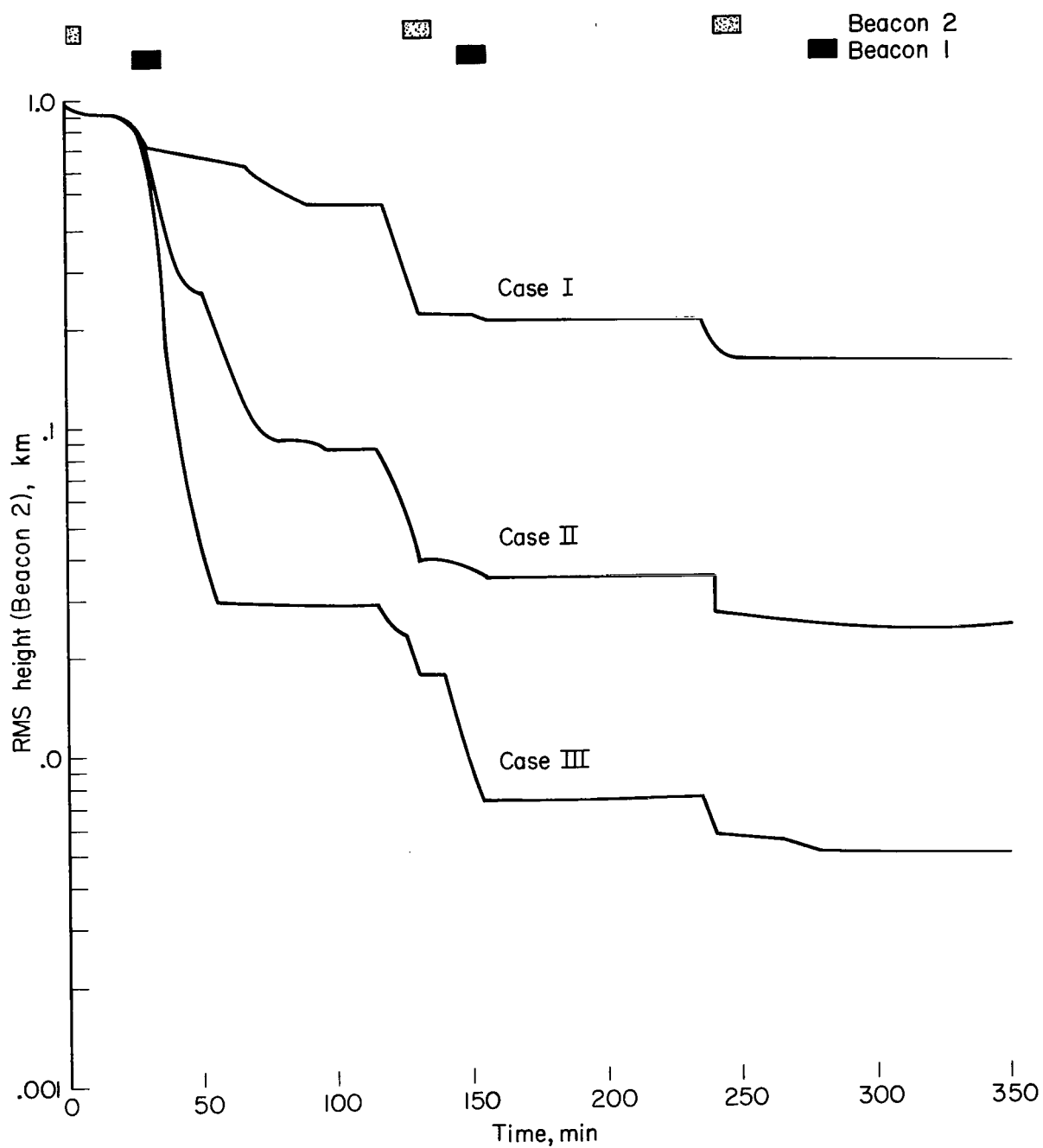
(c) Height improvement.

Figure 8.- Concluded.

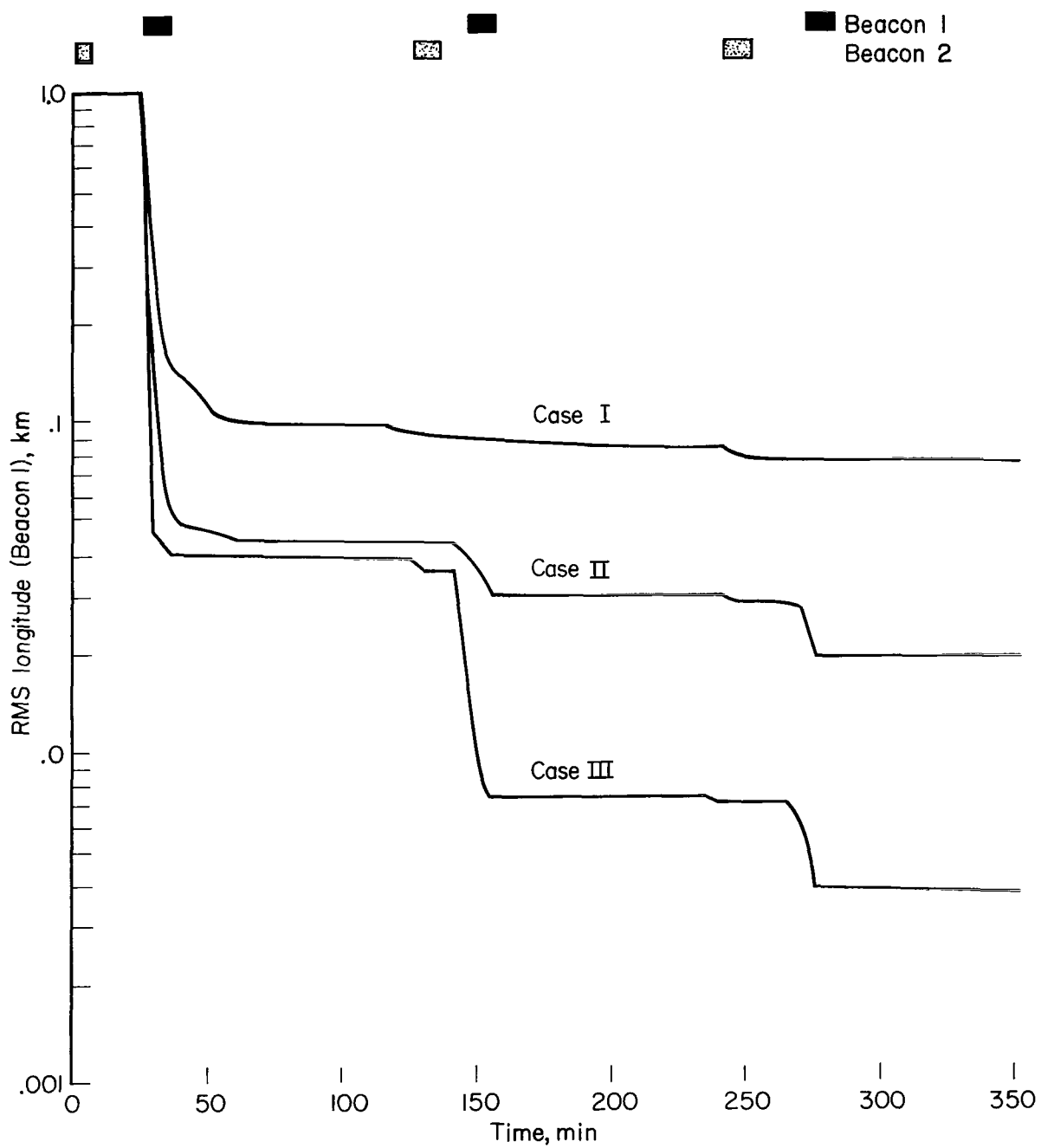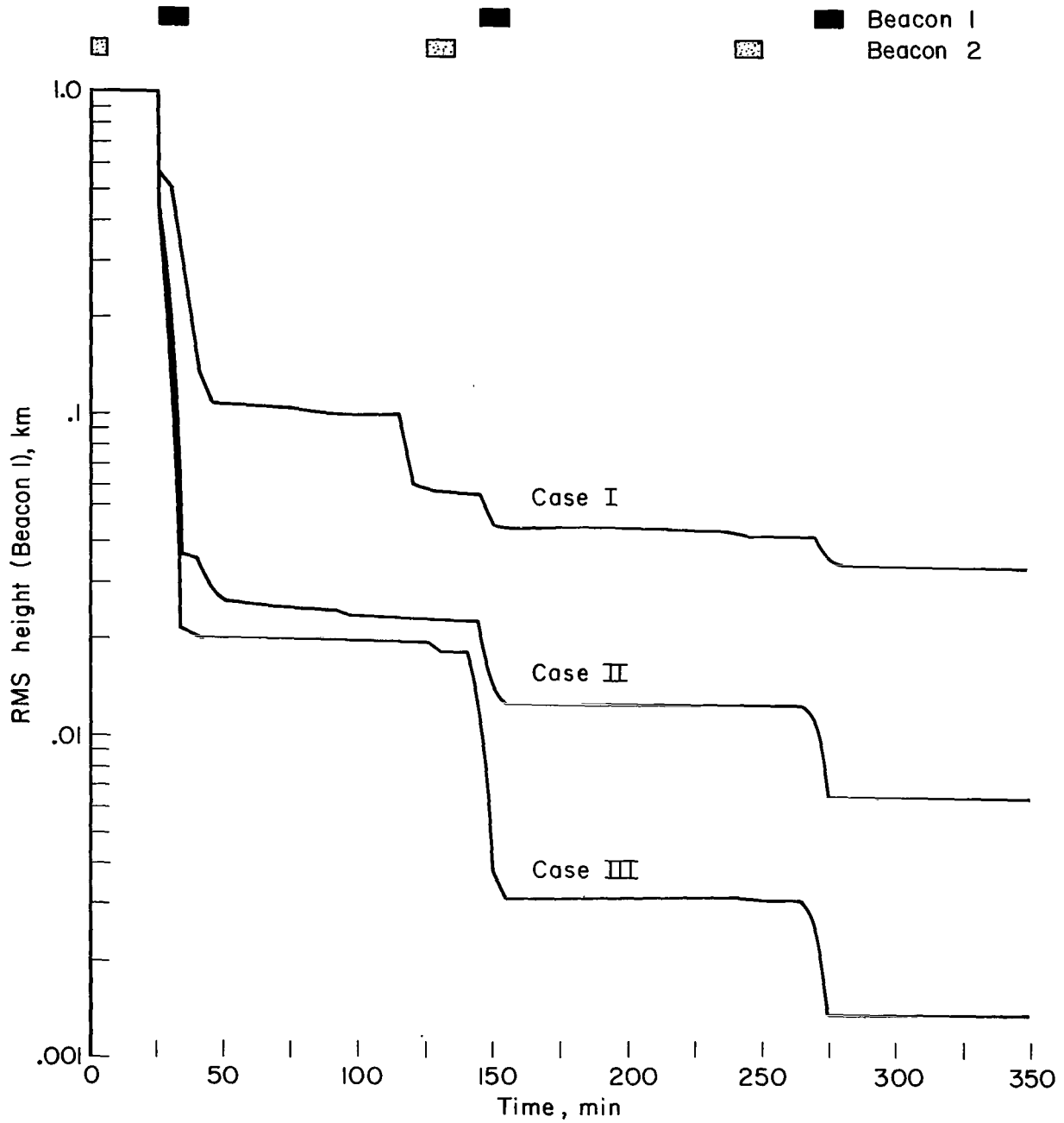| Code	Measurement Accuracy			Initial Beacon Location Errors											
	Earth-based (E)	On-board (OB)		Beacon C′ (C)			Beacon A (A)			Beacon B (B)			Beacon C (C)		
	$\sigma_{\dot\rho}$ (m/s)	$\sigma_{\dot\rho}$ (m/s)	σ_ρ (m)	σ_N(m)	σ_E(m)	σ_D(m)	σ_N(m)	σ_E(m)	σ_D(m)	σ_N(m)	σ_E(m)	σ_D(m)	σ_N(m)	σ_E(m)	σ_D(m)
1	.04	.3		1000	1000	1000	1000	1000	1000	1000	1000	1000	1000	1000	1000
2			30				100	100	100	100	100	100	100	100	100

Goldstone
Woomera
Johannesburg
Beacon C′
Beacon A
Beacon B
Beacon C

Conditions for run

□ E
○ E + OB (1) + OB (2) + C′ (1) + B (1)
◐ E + OB (1) + OB (2) + C′ (1) + A (1)
◇ E + OB (1) + OB (2) + C′ (1) + B (2)
△ E + OB (1) + OB (2) + C′ (1) + A (2)
◑ E + OB (1) + OB (2) + A (2) + C (2)

(a) On-board range and range-rate observations.

Figure 9.- Position estimation error using both earth-based and on-board measurements.

43

| Code | Measurement Accuracy | | | Initial Beacon Location Errors | | | | | |
| | Earth-based (E) | On-board (OB) | | Beacon A (A) | | | Beacon C (C) | | |
	$\sigma_{\dot{\rho}}$ (m/s)	$\sigma_{\dot{\rho}}$ (m/s)	σ_{ρ} (m)	σ_N (m)	σ_E (m)	σ_D (m)	σ_N (m)	σ_E (m)	σ_D (m)
1	.04	.3		1000	1000	1000	1000	1000	1000
2			30	100	100	100	100	100	100

Goldstone
Woomera
Johannesburg
Beacon A
Beacon C

Conditions for run
□ E + OB (1) + OB (2) + A (2) + C (2)
△ E + OB (2) + A (2) + C (2)
○ E + OB (1) + A (2) + C (2)

(b) On-board range or range-rate observations.

Figure 9.- Concluded.

Code	Measurement Accuracy			Initial Beacon Location Errors											
	Earth-based (E)	On-board (OB)		Beacon C' (C')			Beacon A (A)			Beacon B' (B')			Beacon C (C)		
	$\sigma_{\dot{\rho}}$ (m/s)	$\sigma_{\dot{\rho}}$ (m/s)	σ_{ρ} (m)	σ_N(m)	σ_E(m)	σ_D(m)	σ_N(m)	σ_E(m)	σ_D(m)	σ_N(m)	σ_E(m)	σ_D(m)	σ_N(m)	σ_E(m)	σ_D(m)
1	.04	.3		1000	1000	1000	1000	1000	1000	1000	1000	1000	1000	1000	1000
2			30				100	100	100	100	100	100	100	100	100

Beacon B'
Beacon C'
Beacon A
Beacon C

Conditions for run

△ OB (1) + OB (2) + C' (1) + A (1)
○ OB (1) + OB (2) + C' (1) + B' (1)
▽ OB (1) + OB (2) + C' (1) + B' (2)
□ OB (1) + OB (2) + C' (1) + A (2)
◇ OB (1) + OB (2) + C (2) + A (2)

(a) Range and range-rate observations.

Figure 10.- Position estimation error using on-board observations only.

Code	Measurement Accuracy			Initial Beacon Location Errors					
	Earth-based (E)	On-board (OB)		Beacon A (A)			Beacon C (C)		
	$\sigma_{\dot{\rho}}$ (m/s)	$\sigma_{\dot{\rho}}$ (m/s)	σ_{ρ} (m)	σ_N (m)	σ_E (m)	σ_D (m)	σ_N (m)	σ_E (m)	σ_D (m)
1	.04	.3		1000	1000	1000	1000	1000	1000
2			30	100	100	100	100	100	100

Conditions for run

◇ OB (1) + A (2) + C (2)

O OB (2) + A (2) + C (2)

□ OB (1) + OB (2) + A (2) + C (2)

▨ Beacon A
■ Beacon C
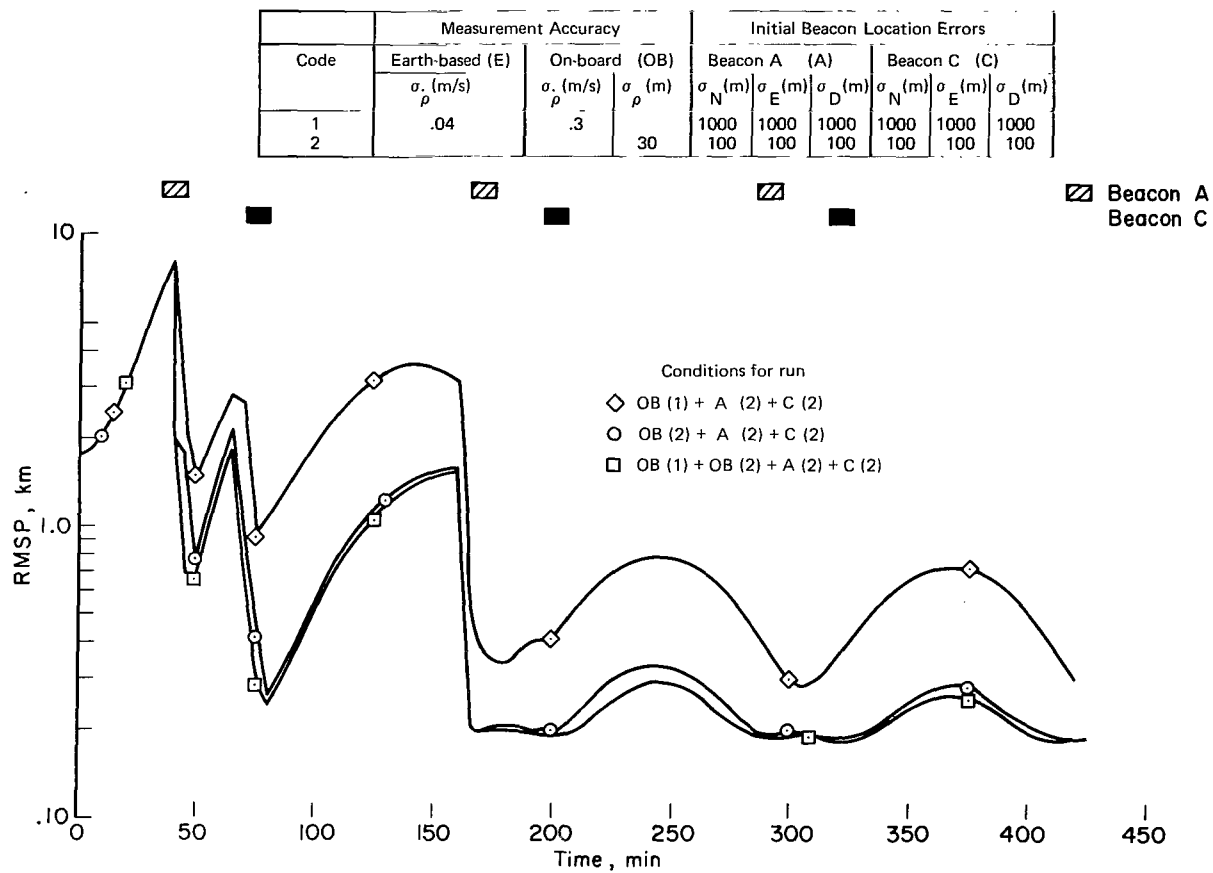
(b) Range or range-rate observations.

Figure 10.- Concluded.

"*The aeronautical and space activities of the United States shall be
conducted so as to contribute . . . to the expansion of human knowl-
edge of phenomena in the atmosphere and space. The Administration
shall provide for the widest practicable and appropriate dissemination
of information concerning its activities and the results thereof.*"

— NATIONAL AERONAUTICS AND SPACE ACT OF 1958

NASA SCIENTIFIC AND TECHNICAL PUBLICATIONS

TECHNICAL REPORTS: Scientific and
technical information considered important,
complete, and a lasting contribution to existing
knowledge.

TECHNICAL NOTES: Information less broad
in scope but nevertheless of importance as a
contribution to existing knowledge.

TECHNICAL MEMORANDUMS:
Information receiving limited distribution
because of preliminary data, security classifica-
tion, or other reasons.

CONTRACTOR REPORTS: Scientific and
technical information generated under a NASA
contract or grant and considered an important
contribution to existing knowledge.

TECHNICAL TRANSLATIONS: Information
published in a foreign language considered
to merit NASA distribution in English.

SPECIAL PUBLICATIONS: Information
derived from or of value to NASA activities.
Publications include conference proceedings,
monographs, data compilations, handbooks,
sourcebooks, and special bibliographies.

TECHNOLOGY UTILIZATION
PUBLICATIONS: Information on technology
used by NASA that may be of particular
interest in commercial and other non-aerospace
applications. Publications include Tech Briefs,
Technology Utilization Reports and Notes,
and Technology Surveys.

Details on the availability of these publications may be obtained from:

SCIENTIFIC AND TECHNICAL INFORMATION DIVISION

NATIONAL AERONAUTICS AND SPACE ADMINISTRATION
Washington, D.C. 20546